Peptidoglycan-Chi3l1 interaction shapes gut microbiota in intestinal mucus layer

Yan Chen[1#], Ruizhi Yang[1#], Bin Qi[1]*, Zhao Shan[1]*

1. Center for Life Sciences, School of Life Sciences, State Key Laboratory of Conservation and Utilization of Bio-resources in Yunnan, Yunnan University, Kunming, China, 650500*Corresponding author

*email: Bin Qi: qb@ynu.edu.cn and Zhao Shan: shanzhao@ynu.edu.cn

# Equally contributed

Abstract

The balanced gut microbiota in intestinal mucus layer plays an instrumental role in the health of the host. However, the mechanisms by which the host regulates microbial communities in the mucus layer remain largely unknown. Here, we discovered that the host regulates bacterial colonization in the gut mucus layer by producing a protein called Chitinase 3-like protein 1 (Chi3l1). Intestinal epithelial cells are stimulated by the gut microbiota to express Chi3l1. Once expressed, Chi3l1 is secreted into the mucus layer where it interacts with the gut microbiota, specifically through a component of bacterial cell walls called peptidoglycan. This interaction between Chi3l1 and bacteria is beneficial for the colonization of bacteria in the mucus, particularly for gram-positive bacteria like *Lactobacillus*. Moreover, a deficiency of Chi3l1 leads to an imbalance in the gut microbiota, which exacerbates colitis induced by dextran sodium sulfate (DSS). By performing fecal microbiota transplantation from Villin-cre mice or replenishing *Lactobacillus* in IEC$^{\Delta Chil1}$ mice, we were able to restore their colitis to the same level as that of Villin-cre mice. In summary, this study shows a "scaffold model" for microbiota homeostasis by interaction between intestinal Chi3l1 and bacteria cell wall interaction, and it also highlights that an unbalanced gut microbiota in the intestinal mucus contributes to the development of colitis.

Key words: Chi3l1, intestinal homeostasis, gut microbiota, peptidoglycan,

Introduction

Intestinal homeostasis is crucial for maintaining human health[1]. Alterations in gut microbiota composition have been linked to various diseases including cancer, obesity, and neurological disorders[2-6]. Dysbiosis, which refers to an imbalance in gut microbiota, is characterized by decreased microbial diversity, the presence of harmful microbes, or absence of beneficial ones [7]. Studies in mice models lacking key components of mucus have shown increased susceptibility to colitis and dysbiosis in the mucosal layer[8]. Therefore, understanding the factors that influence gut microbiota is a fundamental goal in microbiome research[9]. Growing evidence suggests that colonization of the gut mucosal layer can affect the susceptibility and progression of intestinal diseases like inflammatory bowel disease (IBD), irritable bowel syndrome, and celiac disease[10]. Inflammatory bowel diseases, such as Crohn's disease (CD) and Ulcerative Colitis (UC), are characterized by chronic inflammation of the intestinal mucosa. Although the cause of the inflammatory bowel disease is unclear, mouse models lacking the key components of the mucus are predisposed to colitis, accompanied by dysbiosis in mucosa[11, 12], which is in accordance with

increased epithelial-adherent microbial communities in biopsies from patients with IBD [13, 14]. Furthermore, there were significant differences in the gut microbiota of CD patients compared with healthy controls, and these differences were only present in mucosal samples (not stool samples), suggesting that bacteria in the mucosal layer may be more important for the development of IBD[15]. Donaldson et al. discovered that the intestinal flora utilizes host immunoglobulin A (IgA) for mucosal colonization, indicating that the host may secrete certain factors to maintain intestinal flora homeostasis in the mucus[16]. However, the mechanisms regulating gut microbiota colonization in the mucosal layer remain largely unknown. We aim to investigate the regulation of microbial communities in gut mucus and its implications in intestinal diseases.

Chitinase 3-like protein 1 (Chi3l1, also known as YKL-40 in humans) is a secreted protein that belongs to the glycosylhydrolase 18 family[17]. Despite its name, Chi3l1 can bind to chitin but does not have chitinase activity[18]. In our investigation, we noticed that chitin and peptidoglycan, a major component of bacterial cell walls, have similar structures [19]. Based on this information, we speculate that Chi3l1 might also interact with peptidoglycan and, therefore, interact with bacteria. Interestingly, Chi3l1 is expressed in intestinal epithelial cells and the lamina propria. We hypothesize that Chi3l1 may be secreted by intestinal epithelial cells and regulate the gut microbiota through its interaction with peptidoglycan in the mucous layer. In our study, we discovered that gut microbiota induce the expression of Chi3l1 in epithelial cells. Once expressed, Chi3l1 is secreted into the mucosa and interacts with bacteria, particularly with the bacterial cell wall component peptidoglycan. This interaction promotes bacterial colonization, especially of beneficial bacteria such as *Lactobacillus*. As a result, mice with higher levels of Chi3l1 are less susceptible to colitis.

Results

Intestinal epithelial cells express Chi3l1 induced by gut microbiota.

The gut microbiota's composition is shaped by host factors, including IgA [16], RegIIIγ [20], and TLR-5 [19]. Yet, specific host factors which maintain the homeostasis of the microbiota remain largely undefined. Drawing on the theory of co-evolution between the host and microbiota [21], we propose that host factors, which are induced by bacteria in the gut, could play a pivotal role in regulating bacterial colonization and composition. In a previous study, it was observed that both live *E.coli* and heat-killed *E.coli* treatment resulted in a significant increase in the expression of the gene encoding Chi3l1 in human intestinal organoids[22]. To verify this finding, we conducted immunohistochemical staining on intestinal tissue sections of germ-free and specific pathogen free (SPF) C57BL/6J wildtype mice. We observed a substantial increase of Chi3l1 expression in SPF mice compared to germ-free mice (Fig. 1A). The intestinal epithelium comprises various cell types, including intestinal cells, goblet cells, endoentercrine cells, Tuft cells, Paneth cells, M cells, and others [21]. To identify the cellular sources of Chi3l1, we performed co-staining with markers for specific cell types, including Chromogranin A (ChgA) for enteroendocrine cells, Ulex Europaeus Agglutinin I (UEA-1) for goblet cells and Paneth cells, and Double cortin-like kinase 1 (DCLK1) for tuft cells. Our results revealed that Chi3l1 is primarily expressed in enteroendocrine cells in the ileum and goblet or Paneth cells in the colon (Fig. 1B). However, Chi3l1 expression was not observed in tuft cells (Supplementary Figure 1).

Furthermore, we isolated total bacteria from wildtype mouse feces and treated DLD-1 cells (a colorectal adenocarcinoma cell line) with the bacterial extract for 12 hours. We found that the bacterial extract directly induced Chi3l1 expression in DLD-1 cells (Fig. 1C). To examine whether the induction of Chi3l1 expression require a specific bacteria strain, we further identified the bacterial extract using 16S rRNA sequencing. Our results revealed that *E.coli* specifically stimulated Chi3l1 expression in DLD-1 cells, while *Staphylococcus Sciuri* did not have the same effect (Fig. 1D). Next, we wondered what component of bacteria can induce Chi3l1 expression. We tried heat-killed *E.coli*, which maintains bacterial cell wall integrity. We found that treatment of DLD-1 cells with heat-killed *E.coli* also led to an induction of Chi3l1 expression (Fig. 1E). These findings suggest that the induction of Chi3l1 expression does not necessarily require live bacteria and that bacterial components alone are sufficient to induce this response. To further investigate the specific bacterial component responsible for Chi3l1 induction, we tested lipopolysaccharides (LPS), a classical component of *E.coli*. Our results showed that LPS treatment of DLD-1 cells can induce Chi3l1 expression (Fig. 1F&G). Collectively, these findings provide evidence that the gut microbiota can induce Chi3l1 expression in intestinal epithelial cells.

Chi3l1 interact with bacteria via peptidoglycan.

Chi3l1 belongs to a group of proteins called non-enzymatic chitinase-like proteins, which are known to bind chitin. Chitin is a polysaccharide present in the exoskeleton of arthropods and the cell walls of fungi[23]. By comparing the structure of chitin with that of peptidoglycan (PGN), a component of bacterial cell walls, we observed that they have similar structures (Fig. 2A). Based on this observation, we hypothesized that Chi3l1 may interact with gut bacteria through PGN. To test our hypothesis, we conducted co-incubation experiments where we mixed recombinant mouse Chi3l1 (rmChi3l1) with either Gram-positive or Gram-negative bacteria and then precipitated the bacteria through centrifugation. We found that rmChi3l1 was present in the pellet obtained from both Gram-positive and Gram-negative bacteria (Fig. 2B), suggesting that Chi3l1 can directly interact with bacteria.

To further investigate the interaction between Chi3l1 and PGN, we also co-incubated PGN with rmChi3l1 and precipitated the PGN through centrifugation. PGN is an insoluble substance and hence can be precipitated by centrifugation. Consistent with our previous results, we observed that rmChi3l1 was present in the pellet obtained from PGN but not in the pellet obtained from bovine serum albumin (BSA), which served as a negative control (Fig. 2C). Furthermore, we also examined the interaction between PGN and recombinant human Chi3l1 (rhChi3l1) and obtained similar results (Fig. 2D). These findings indicate that Chi3l1 interacts with bacteria through PGN.

Intestinal bacteria are disordered in IEC$^{\Delta Chil1}$ mice, especially Gram-positive bacteria.

To gain initial insights into how the expression of Chi3l1 in intestinal epithelial cells (IECs) affects the colonization of gut microbiota, we created mice with a specific deficiency of Chi3l1 in IECs (referred to as IEC$^{\Delta Chil1}$ mice) (Supplementary Figure 2). We then conducted bacterial 16S rRNA sequencing analysis of the colon contents of both Villin-cre and IEC$^{\Delta Chil1}$ littermates. Our analysis

of alpha diversity revealed that the bacterial population was relatively lower in IEC$^{\Delta Chil1}$ littermates compared to Villin-cre littermates (Figure 3A). This finding was further confirmed by conducting universal bacterial 16S rRNA qPCR analysis of the feces and ileum contents of IEC$^{\Delta Chil1}$ and Villin-cre littermates, which also showed lower bacterial enrichment in IEC$^{\Delta Chil1}$ mice (Figure 3B). Furthermore, principal component analysis demonstrated significant differences in bacterial diversity between Villin-cre and IEC$^{\Delta Chil1}$ littermates (Figure 3C).

When we examined the relative abundance of Gram-positive and Gram-negative bacteria between Villin-cre and IEC$^{\Delta Chil1}$ littermates, we observed that Gram-positive bacteria were significantly reduced in IEC$^{\Delta Chil1}$ mice, while there was no notable difference in Gram-negative bacteria (Figure 3D). This result was further validated by staining lipoteichoic acid (LTA), a component present on Gram-positive bacteria, which revealed a lower abundance of Gram-positive bacteria in IEC$^{\Delta Chil1}$ compared to Villin-cre littermates (Figure 3E). Moreover, visualization of *Firmicutes* by bacteria FISH staining, a dominant group of Gram-positive bacteria in the gut, also showed reduced levels of *Firmicutes* in the colon lumen of IEC$^{\Delta Chil1}$ mice compared to Villin-cre mice (Figure 3F). Analysis of the relative abundance of specific Gram-positive bacterial species demonstrated a significant reduction in *Lactobacillus* in IEC$^{\Delta Chil1}$ mice compared to Villin-cre mice (Figure 3G). Similar results were observed in Chil1$^{-/-}$ mice compared to wildtype mice (Figure 3H). These findings suggest that Chi3l1 plays a role in regulating the colonization of Gram-positive bacteria, particularly *Lactobacillus*, in the murine gut.

Chi3l1 promotes the colonization of Gram-positive bacteria in intestinal mucus.

Chi3l1 was found in secretory cells like goblet cells and Paneth cells, suggesting that it may be secreted into the intestinal lumen (Fig. 1B). Immunohistochemistry staining of Chi3l1 in the colon revealed a large amount of Chi3l1 signals in the mucus layer (Fig. 4A). Immunofluorescence co-staining of Chi3l1 with UEA-1 in the colon yielded similar results (Fig. 4B). Furthermore, Chi3l1 was also detected in the ileum and colonic tissues and mucus layer (Fig. 4C&D). These findings indicate that mouse Chi3l1 is specifically expressed in intestinal secretory epithelial cells and secreted into the intestinal lumen. Since large amounts of Chi3l1 is secreted into the mucus and Chi3l1 interact with bacteria, we hypothesize that Chi3l1 may regulate the colonization of Gram-positive bacteria in the mucus layer. To test this hypothesis, we isolated bacterial DNA from the ileum and colon mucus of both wildtype and Chi1l$^{-/-}$ mice. Quantification of Gram-positive bacteria and *Lactobacillus* using qPCR revealed that both the ileum and colon mucus of Chi1l$^{-/-}$ mice had significantly lower levels of Gram-positive bacteria and *Lactobacillus* compared to that of wildtype mice (Fig. 4E&F).

To further validate these results, we labeled a Gram-positive bacteria strain, *E. faecalis*, with fluorescent D-amino acids (FDAA), which can metabolically label bacterial peptidoglycans[24]. We then performed rectal injection of both wildtype and Chi1l$^{-/-}$ mice with FDAA-labeled *E. faecalis*. The data demonstrated that Chi1l$^{-/-}$ mice had much lower colonization of *E. faecalis* compared to wildtype mice (Fig. 4G). Based on these findings, we conclude that Chi3l1 promotes the colonization of Gram-positive bacteria, particularly *Lactobacillus*, in the intestinal mucus. Additionally, we also observed that the deletion of Chi3l1 significantly reduced mucus layer

thickness, which may be attributed to the disrupted colonization of Gram-positive bacteria in the intestinal mucus layer (Supplementary Figure 3 A&B).

Disordered intestinal bacteria in IEC$^{\Delta Chil1}$ mice contribute to colitis.

From the above data, it is evident that Chi3l1 is secreted into the intestinal mucus to influence the colonization of Gram-positive bacteria, particularly *Lactobacillus*. We are now interested in understanding the role of Chi3l1-regulated microbiota in a pathological condition. We observed a significant increase in *Chil1* mRNA expression in the colon tissues of patients with either Crohn's disease (CD) or Ulcerative colitis (UC) compared to normal tissues (Fig. 5A). To investigate further, we created a colitis mouse model by subjecting Villin-cre and IECΔChil1 mice to a 2% dextran sulfate sodium (DSS) diet for 7 days (Fig. 5B). The severity of colitis was assessed based on weight loss, colon length, and tissue damage. Without the DSS challenge, the colon length and structure were similar between Villin-cre and IEC$^{\Delta Chil1}$ mice (Fig. 5D&E). However, upon DSS challenge, the IEC$^{\Delta Chil1}$ mice showed significantly shorter colon length, faster body weight loss, and more severe inflammation compared to the Villin-cre mice (Fig. 5C-E).

To rule out the effects of Chi3l1 on the host contributed to colitis, we pretreated the mice with antibiotics to eliminate gut microbiota before inducing colitis (Supplementary Figure 4A). The Universal bacterial 16S rRNA qPCR data indicated that the majority of gut microbiota were eliminated after antibiotics treatment (Supplementary Figure 4B). However, the IEC$^{\Delta Chil1}$ mice exhibited a milder colitis phenotype, including slower body weight loss, longer colon length, and less inflammation compared to the Villin-cre mice (Supplementary Figure 4C-E). We believe that this could be due to the relationship between Chi3l1 and inflammation. Based on these findings, it is apparent that Chi3l1's effects on gut microbiota play a more significant role in colitis.

To further elucidate the role of Chi3l1-regulated gut microbiota in colitis, we conducted fecal microbiota transplantation (FMT) and *Lactobacillus reuteri* transplantation experiments. We first eliminated gut microbiota through a 10-day course of antibiotics and then performed FMT from Villin-cre mice or administered oral gavage of *Lactobacillus reuteri* to IEC$^{\Delta Chil1}$ mice for 2 weeks, followed by a 7-day period of 2% DSS feeding (Fig 5F). FMT partially restored the colon length of IEC$^{\Delta Chil1}$ mice to that of Villin-cre mice after the DSS challenge, but did not have an impact on body weight loss or the level of inflammation in the gut (Fig. 5G-I). IEC$^{\Delta Chil1}$ mice transplanted with *Lactobacillus* displayed a similar colitis phenotype as Villin-cre mice, characterized by similar weight loss, colon length reduction, and gut inflammation (Fig. 5G-I). These findings further validate the notion that Chi3l1-regulated gut microbiota, especially *Lactobacillus*, offers protection against colitis.

Discussion

The intricate relationship between gut bacteria and their host organisms plays a crucial role in maintaining health. Key to this relationship are the processes of co-evolution and co-speciation, which help maintain balance within the gut microbiota community. Understanding how the host influences these bacterial communities is critical to comprehend the complex interplay between host and gut bacteria. In this study, we uncovered the direct interaction between Chi3l1 and gut

microbiota via bacterial cell wall component-peptidoglycan, thereby helping mucous colonization of gut microbiota, especially Lactobacillus, which is beneficial for host against colitis (Fig. 6). Furthermore, the “scaffold model” of host Chi3l1 directly interacting with microbial PGN, as reported in our study, could significantly enhance our understanding of the mechanisms through which other bacteria colonize the gut.

Several studies have suggested a potential correlation between Chi3l1 and bacteria. For instance, it has been demonstrated that Chi3l1 is produced by intestinal epithelial cells in enteritis disease and aids in the elimination of pathogenic bacteria in the gut by neutrophils[25]. Another study observed an increase in Chi3l1 expression in mammary tissues of dairy cows infected with pathogenic E. coli, which promoted the recruitment of neutrophils[26]. Furthermore, Chi3l1 was found to be induced during *Streptococcus pneumoniae* infection, where it enhanced bacterial elimination by preventing the death of lung macrophages and improving host tolerance[27]. Additionally, a study in mouse colonic epithelial cells showed that Chi3l1 enhances bacterial infection and adhesion[28]. However, the specific mechanism underlying the relationship between Chi3l1 and the gut microbiota has not been fully explored, likely due to a lack of Chi3l1-specific knockout mice. Here, by using intestinal Chi3l1-specific knockout mice, we demonstrated a new function of Chi3l1 in gut, which shapes bacterial colonozation through direct interaction with bacterial cell wall component, PGN. Moreover, Chi3l1-regulated gut microbiota, especially *Lactobacillus*, offers protection against colitis.

In our study, we demonstrated that heat-killed bacteria can induce the expression of Chi3l1 in intestinal epithelial cells (Fig. 1E). This suggests that the component of the bacterial cell wall is sufficient to induce Chi3l1 expression. The bacterial cell wall is a complex structure mainly composed of peptidoglycan, but it may also contain other components such as teichoic acids and lipoteichoic acid in gram-positive bacteria, or an outer membrane containing various polysaccharides, lipids, and proteins in gram-negative bacteria[29]. Our findings indicated that lipopolysaccharide (LPS), a component of the bacterial cell wall, can slightly increase Chi3l1 expression (Fig. 1F&G), but higher levels of LPS do not further enhance Chi3l1 expression (data not shown). This suggests that there might be other components of the cell wall that can induce Chi3l1 expression in intestinal epithelial cells.

Peptidoglycan, which is a major component of the bacterial cell wall, is composed of polysaccharide chains alternating with N-acetylglucosamine (NAG) and N-acetylmuramic acid (NAM). These chains are crosslinked through a tetrapeptide[29]. We showed that Chi3l1 can directly interact with peptidoglycan (Fig. 2C&D). Given the structural similarity between chitin and peptidoglycan (Fig. 2A), it is likely that Chi3l1 binds to the polysaccharide chains rather than the tetrapeptide in peptidoglycan. Previous studies have investigated the crystal structure of human Chi3l1 in complex with chitin, revealing a binding groove with different subsites for chitin fragments[30]. Other studies have also identified specific amino acids in chitinases that play a key role in the interaction with chitin[31, 32]. Nevertheless, further investigation is necessary to better understand the binding sites in Chi3l1 for peptidoglycan.

In the colon, there are two distinct parts of the mucus layer. The inner layer is attached and has a low number of microbes, while the outer layer is looser and densely populated by microorganisms. [33]. The diversity of bacteria in the mucus layer is similar to that found in the gut lumen[34]. Our study found that mice lacking the Chi3l1 gene had fewer Gram-positive bacteria, particularly *Firmicutes* and *Lactobacillus*, compared to normal mice (Fig. 3F-H). This was confirmed by qPCR data (Fig. 4E&F). However, not all Gram-positive bacteria were reduced in these mice, as we found an increase in *Turicibacter* in the colon (Fig. 3G) and feces (data not shown). We believe this may be due to a combined effect of the host and gut microbiota. Another important factor for microbial growth in the colon is the integrity of the mucus barrier[12].We noticed a thinning of the mucus barrier in the mice lacking Chi3l1 compared to normal mice (Supplementary Figure 3 A&B). However, we did not observe an increase in mucin-degrading bacteria such as *Bacteroides* or *Allobaculum*[35, 36] or a decrease in mucin-producing cells in these mice. We think that there may be bacteria that aid in the formation of the gut mucus, and these bacteria are decreased in mice lacking Chi3l1.

In patients with inflammatory bowel disease (IBD), the density and diversity of the microbial community in the intestines are reduced. Specifically, there is a decrease in *Firmicutes* and an increase in *Bacteroides* and facultative anaerobic bacteria like *Enterobacteriaceae*[37]. However, the cause of colitis in IBD is still a subject of debate. Our data shows that a deficiency of Chi3l1 in intestinal epithelial cells leads to dysbiosis (Fig. 3). Mice without Chi3l1 are more susceptible to colitis induced by dextran sulfate sodium (DSS) compared to normal mice (Fig. 5B-E). However, when we transplanted fecal microbiota from normal mice or supplemented with *Lactobacillus reuteri* in mice without Chi3l1, DSS-induced colitis was significantly reduced (Fig. 5F-I). These results suggest that disruptions in the gut microbiota contribute to colitis. In summary, our study demonstrates that bacterial challenge induces the expression of Chi3l1 in intestinal epithelial cells. Once produced, Chi3l1 is released into the mucus layer where it interacts with the gut microbiota, particularly through peptidoglycan, a primary component of bacterial cell walls. This interaction is beneficial for the colonization of bacteria, especially gram-positive bacteria like *Lactobacillus*, in the mucus layer. Dysbiosis resulting from a lack of Chi3l1 exacerbates DSS-induced colitis, highlighting the role of dysbiosis as a contributing factor to colitis.

Methods

Animal experiments and procedures.

C57BL/6J (Strain No. N000013), Germ-free (Strain No. N000295), Chil1$^{fl/fl}$ (Strain No. T013652), Chil1$^{-/-}$ (Strain No. T014402) mice were purchased from GemPharmatech. Villin-cre mice were provided by Dr. Qun Lu (Yunnan University, China,). All mouse colonies were maintained at the animal core facility of Yunnan University. C57BL/6J was used as wildtype control since Chil1$^{-/-}$ mice are on the C57BL/6J background, as determined by PCR (data not shown). The animal studies described have been approved by the Yunnan University Institutional Animal Care and Use Committee (IACUC, Approval No. YNU20220256). Female mice aged 8-10 weeks old were used in most studies.

Genotyping First, place the tail clippings into 1.5ml tubes. Then, transfer 75uL of the master mix solution (composed of 60uL H2O, 7.5uL 250mM NaOH, and 7.5uL 2mM EDTA) into the tubes with the tail clippings. Next, place the tubes in a thermocycler and incubate them at 98°C for 1 hour. After that, lower the temperature to 15°C and add 75uL of neutralization buffer (consisting of 40mM Tris HCl, pH=5.5). Following the addition of Tris HCl, centrifuge the tubes at 4000rpm for 3 minutes. Then, create a 1:10 dilution by transferring 2μl of the supernatant to a new 0.2mL tube and adding 18uL of water. This diluted solution can be utilized in the genotyping PCR reaction. Prepare a total of 25μl PCR reaction mix, composed of 12.5 μl 2x Taq Master Mix, Dye plus (Vazyme P112-03), 1μl of each primer, 2 μl of template, and add H2O to reach a total volume of 25μl. Conduct the PCR reaction on a Biorad PCR machine, following the programmed steps: 1. 95°C for 5 minutes, 2. 98°C for 30 seconds, 3. 65°C with a decrement of 0.5°C per cycle for 30 seconds, 4. 72°C for 45 seconds, repeat steps 2-4 for a total of 20 cycles, 5. 98°C for 30 seconds, 6. 55°C for 30 seconds, 7. 72°C for 45 seconds, repeat steps 5-7 for a total of 20 cycles, 8. 72°C for 5 minutes, and finally, 9. hold at 10°C. Primer sequences are provided in table S1.

Table S1

Aim genes	PCR No.	Primer No.	Sequence	Band Size
flox	① 5'arm (flox)	F1(JS05000-Chil1-5wt-tF1)	CTTGTTCAGCCAAGGTGATGGGTA	WT:270bp targeted:375bp
		R1(JS05000-Chil1-5wt-tR1)	CTACCTGATTGCTGGGGCTCATTA	
	② 3'arm	F2(JS15000-Chil1-3wt-F1)	CCAGTATTTAGAGGCAGAGAGATGGTG	WT:283bp targeted:384bp
		R2(JS15000-Chil1-3wt-R1)	CTCGAATTCAGAAATCTGCCTGCCT	
Chil1$^{-/-}$	①	F1(JS05000-Chil1-5wt-tF1)	CTTGTTCAGCCAAGGTGATGGGTA	WT: 2960 bp Targeted: ~256 bp
		R1(JS05000-Chil1-3wt-tR1)	CTCGAATTCAGAAATCTGCCTGCCT	
	②	F2(JS15000-Chil1-wt-F1)	CTGTTAGTTGCACCTTGGAGCAGTCA	WT: 309 bp Targeted:0 bp
		R2(JS15000-Chil1-wt-R1)	CAGATATAGGAGAACATCCAGTCTGGG	
Chil1-reporter	①	EGE-YQH-063-A-WT-F	CAGTTTCCCAACCCCTCACCTC	Targeted:485 ~bp
		EGE-YQH-063-A-Mut-R	AAGAAGTCGTGCTGCTTCATGTGGT	
	②	EGE-YQH-063-A-WT-F	CAGTTTCCCAACCCCTCACCTC	WT:323 Targeted:1106~bp
		EGE-YQH-063-A-WT-R	CTACCCTAGTTCCCTGTTCTCCA	
Cre	Cre①	Cre1	AGGTTCGTTCACTCATGGA	Cre:250bp Internal Control (Fabpi)=480bp
		Cre2	TTCGACCAGTTTAGTTACCC	
	IntC500②	IntC500F	CCTCCGGAGAGCAGCGATTAAAAGTGTCAG	

		IntC500R	TAGAGCTTTGCCACATCACAGGTCATTCAG	

Rectal administration of FDAA-labeled E. faecalis For FDAA-labeled *E. faecalis*, *E. faecalis* were grown in LB media until reaching mid-exponential phase, approximately 4 hours. FDAA was then added to the culture media to a final concentration of about 17 μM. The *E. faecalis* continued to grow for 4 hours and were then harvested by centrifugation (5000 x g for 10 min), washed, and resuspended in PBS at a density of $5x10^9$ CFU/ml. For rectal administration, wildtype and Chil1$^{-/-}$ mice were fasted overnight (5:00pm to 9:00am) before intraperitoneally (i.p.) injecting them with 400mg/kg tribromoethanol (Nanjing AIBI BioTechnology, M2910), followed by rectal injection of $1x10^9$ FDAA-labeled E. faecalis in 200 μl PBS via a flexible catheter. The catheter was inserted into the anus to a depth of 4.5 cm, and the *E. faecalis* were injected slowly to avoid overflow. The mice were then kept upside down for approximately 2 minutes. After 4 hours of rectal injection, the mice's colons were collected and immediately embedded in OTC embedding medium for observation on 5μm thick frozen sections.

DSS-induced mouse colitis Villin-cre and IEC$^{\Delta Chil1}$ mice were fed a 2% dextran sodium sulfate (DSS, MP, 9011-18-1) solution in their drinking water for 7 days. The mice's body weight was monitored daily during the feeding period. After the 7-day DSS treatment, the mice were sacrificed. Colons were collected, and their length was measured from the cecum to the rectum. Colon paraffin sections were harvested, and H&E staining was performed to examine gut inflammation.

Antibiotics treatment IEC$^{\Delta Chil1}$ mice were fed an antibiotics mixture containing 0.5 mg/ml of Metronidazole (Solarbio, M8060), 1 mg/ml of vancomycin (Solarbio, V8050), 1 mg/ml of Ampicillin (Solarbio, A8180), and 0.5 mg/ml of Neomycin Sulfate (Solarbio, N8090) in their drinking water for 7 days (approximately 5ml per mouse per day). After the 7-day antibiotics treatment, the mice were orally gavaged with 200μl of the antibiotics mixture for another 3 days. Microbiota depletion was examined in feces using 16S rRNA qPCR on the 10th day of antibiotics feeding.

Fecal microbiota transplantation (FMT) Fresh feces were collected from 8-10 weeks old Villin-cre mice and immediately snap-frozen in liquid nitrogen. On the experimental day, feces were dissolved in PBS to a concentration of 200 mg/ml and centrifuged at 350g for 5 minutes to collect the supernatant. Antibiotics pre-treated IEC$^{\Delta Chil1}$ mice were orally gavaged with 10 μl of the dissolved feces per gram of mouse weight for 14 days.

Oral gavage of Lactobacillus reuteri *Lactobacillus reuteri* was grown in MRS broth at 37°C for 48 hours under anaerobic conditions. The bacteria were harvested by centrifugation (5000 x g for 10 min), washed, and resuspended in PBS at a density of OD_{605}=1.2-1.3/ml. Antibiotics pre-treated IEC$^{\Delta Chil1\ mice}$ were orally gavaged with 200μl of the dissolved Lactobacillus reuteri per mouse for 14 days.

Bacterial colony identification

Fresh feces were collected from 8-week-old wild-type mice and dissolved in LB culture medium.

The dissolved feces were then cultured at 37°C for 12 hours and plated onto LB agar plates. The grown colonies were picked using sterile pipette tips and resuspended in 20 μl of sterile water. A PCR reaction was performed using 2 μl of the bacterial suspension as template DNA and universal bacterial 16S rRNA primers (27F, 5'-AGAGTTTGATCCTGGCTCAG-3' and 1492R, 5'-GGTTACCTTGTTACGACTT-3') with reaction conditions: 95°C for 5 min followed by 35 cycles of 95°C for 30sec, 55°C for 30sec, 72°C for 2min and then 72°C for 20min. The amplicons were then sequenced, and the resulting sequences were analyzed using BLASTN and the NCBI database for species identification.

Treatment of DLD-1 cells with live, heat-killed bacteria or LPS

Bacteria harvested from mouse feces or specific strains were grown in LB medium at 37°C for 12 hours under aerobic conditions. The bacteria were then collected by centrifugation (5000 x g for 10 min), washed, and resuspended in PBS at a density of 1.2 x 10^{10} CFU/ml. Live bacteria were used directly, while heat-killed bacteria required further heating at 80°C for 30 minutes. DLD-1 cells were grown in DMEM medium supplemented with 10% FBS. Prior to treatment, the cells were replated and allowed to reach 80% confluency. Either live or heat-killed bacteria were added to the cells at a multiplicity of infection of 20 each well, and 100 pg/ml LPS treatment(Sigma, L4392; diluted in PBS) was also performed. After 12-hour incubation, cellular proteins were extracted for western blot analysis or the cells were subjected to immunofluorescent staining.

Bacterial or peptidoglycan binding assay

Different bacteria strains were grown in LB medium at 37°C for 12 hours under aerobic conditions. The bacteria were collected by centrifugation (5000 x g for 10 min), washed, and resuspended in MES buffer (25mM MES, 25mM NaCl, Ph=6.0) at a density of 5x10^9 CFU/ml. 1μg Recombinant mouse Chi3l1 (rmChi3l1) was added to the bacterial suspension and incubated at 4°C under rotation overnight. Supernatant, wash fractions, and bacterial-bound fractions were collected and analyzed using western blot analysis. For the peptidoglycan binding assay, 1μg rmChi3l1 or recombinant human Chi3l1 (rhChi3l1) and bovine serum albumin (BSA) was incubated with 100μg peptidoglycan (PGN). The incubation and wash procedure were similar to the bacterial binding assay, and the proteins in each fraction were analyzed using silver staining or western blot.

Hematoxylin/eosin(H&E) and Periodic acid-Schiff and Alcian blue (AB-PAS) staining

Tissues were fixed with buffered 10% paraformaldehyde (BI, E672001-0500) overnight at 4°C and embedded in paraffin. Ultra-thin tissue slices (5μm) were prepared and deparaffinized. H&E staining was performed on the tissue sections, and slides were examined under a microscope (Leica). For AB-PAS staining, tissues were fixed in Carnoy's solution (60% Ethanol，30% Chloroform，10% Acetic Acid) for 24 hour at 4°C and embedded in paraffin. AB-PAS staining (Solarbio, G1285) was performed according to the manufacturer's protocol. The staining was visualized under the microscope (Leica).

Immunohistochemical (IHC) and immunofluorescent (IF) staining

Tissue paraffin sections were prepared as previously described for H&E staining. Antigen retrieval was performed by treating the sections with citric acid (pH 6.0) at 95°C for 15 minutes, followed by cooling to room temperature. The sections were then washed with PBS and ddH2O. To block

any nonspecific binding, a blocking buffer containing 5% goat serum, 3% BSA, and 0.1% Triton X-100 in PBS was applied to the sections for 1 hour at room temperature in a humidity chamber. The sections were then incubated with anti-Chi3l1 primary antibodies (Invitrogen, PA5-95897, 1:200), followed by staining with Goat anti-Rabbit IgG (H+L) Secondary Antibody-Biotin (Invitrogen, 65-614, 1:2000). Finally, the sections were stained with Horseradish Peroxidase conjugate antibody (Invitrogen, A2664, 1:2000) and developed with DAB for 10 minutes. The slides were examined under a microscope (Leica).

Immunofluorescent staining was also performed on paraffin sections using specific primary antibodies. These included anti-MUC2 (Invitrogen, PA5-103083, 1:50), anti-Chi3l1 (Abcam, ab180569, 1:400; antigen retrieval with Tris-EDTA at pH 9.0), anti-ChgA (Santa Cruz, sc-393941, 1:200; antigen retrieval with citrate at pH 6.0), anti-UEA-1-FITC (GeneTeX, GTX0151, 1:200; antigen retrieval with citrate at pH 6.0), and anti-LTA (Invitrogen, MA1-7402, 1:50). The secondary antibodies used were 488-conjugated Affinipure Goat Anti-Rabbit IgG(H+L) (Jackson ImmunoResearch, 111-545-003, 1:1000) and 594-conjugated Goat Anti-Mouse IgG (H+L) (Jackson ImmunoResearch, 115-585-003, 1:1000). Slides were washed and mounted with antifade medium (Vectashield, H-1000-10). Nuclei were stained with DAPI (Beyotime, c1006, prediluted). Images were captured using a fluorescence microscope (Leica, 2084 DP-80).

Immunofluorescent staining on DLD-1 cells, cells were seeded on coverslips in 12-well plate and challenged with 100 pg/ml LPS (Sigma, L4391; diluted in PBS) for 12 hours. Cells were washed with cold-PBS twice gently, then fixed with 2% paraformaldehyde in PBS at room temperature for 10 min. After removal of fixation buffer and wash twice with cold-PBS, cells were blocked with blocking buffer (3% BSA, 0.5% Triton-X-100 in PBS) for 1 hour in humidity chamber at room temperature. Rabbit anti-Chi3l1 antibody (Proteintech, 12036-1-AP; 1:200) was applied at room temperature for 1 hour. After wash with 1 x TBST three times, secondary antibody AlexaFluor 488 (Jackson ImmunoResearch, 111-545-003, 1:1000) was applied for another 1 hour at room temperature in a humidified chamber under darkness. Finally, cells were counterstained with DAPI (beyotime, C1006) and mounted onto slides. Images were captured using an Olympus BX53F2 microscope.

Fluorescence in situ hybridization (FISH)

Murine intestinal paraffin sections were prepared according to the previously described method for H&E staining. The tissues sections were rehydrated using a graded ethanol series and then washed with distilled water. The gram-positive bacterial probe, consisting of three different sequences (/5Alex550N/TGGAAGATTCCCTACTGC/3AlexF550N/, /5Alex550N/CGGAAGATTCCCTACTGC/3AlexF550N/, /5Alex550N/CCGAAGATTCCCTACTGC/3AlexF550N/), or the control nonspecific probe (/5Alex550N/ACTCCTACGGGAGGCAGC/3AlexF550N/), was diluted to a concentration of 100 nM in FISH hybridization buffer (containing 20 mM Tris pH 7.2, 0.9 M NaCl, and 0.1% SDS) and applied to the slides. The slides were then incubated overnight at 56°C in a humidified chamber. Following incubation, the slides were washed and the nuclei were counterstained with DAPI. The images were captured using a fluorescence microscope (Leica, 2084 DP-80).

Immunoblot and silver staining

Protein extraction from cultured cells involved lysing the cells in 2% SDS lysis buffer, which is prepared by dissolving 2g of SDS powder in 100ml of sterilized ddH2O. Bacteria or peptidoglycan precipitates were resuspended in MES buffer, which contained 25mM MES, 25mM NaCl, and had a pH of 6.0. For protein extraction from mice ileum and colon tissues, 30mg of snap-frozen tissues were homogenized in 1ml of RIPA buffer, which contained 10mM Tris-HCl (pH 8.0), 1mM EDTA, 0.5mM EGTA, 1% TritonX-100, 0.1% sodium deoxycholate, 0.1% SDS, 140mM NaCl, 1mM PMSF, and a proteinase inhibitor. The lysates were then supplemented with 5x SDS loading buffer to a final concentration of 1x. The resulting mixture was subsequently boiled at 100°C for 10 minutes and centrifuged at 4°C and 12,000 rpm for 10 minutes. The supernatants were collected for western blot analysis. The supernatants were separated using a 10% SDS-PAGE gel and then transferred to a polyvinylidene fluoride membrane. The membranes were blocked with 5% nonfat milk in TBST buffer (containing 0.1% Tween-20 in tris-buffered saline) and sequentially incubated with primary antibodies and appropriate horseradish peroxidase (HRP)-conjugated secondary antibodies. Protein bands were detected using enhanced chemiluminescence (ECL) reagent with a Minichemi Chemiluminescence Imaging System. The primary antibodies used included anti-Chi3l1 (RD, MAB2649, 1:2000) and anti-alpha-Actinin (Cell Signaling, 69758S, 1:1000). The secondary antibodies used were goat anti-Rat-IgG (Cell Signaling, 7077s, 1:1000) and goat anti-mouse (Invitrogen, 62-6520, 1:1000). For silver staining, the PAGE gel was subjected to silver staining using a fast-silver staining kit (Beyotime, P0017S) following the manufacturer's instructions.

DNA extraction for 16S rRNA analysis

For isolation of luminal contents from murine ileum and colon, a 9 cm section of ileum and 3 cm section of colon were cut open longitudinally, and luminal contents were scratched off into a pre-weighed 2-ml sterile freezing vial. The weight of the contents was recorded for further processing. For isolation of mucus from murine ileum and colon, tissues were flushed with 2 ml of ice-cold PBS into a pre-weighed 2-ml sterile freezing vial after removal of the liminal contents. The mucus was then pelleted by centrifugation at 10,000g for 10 minutes, and the supernatant was removed. For feces isolation, fresh murine feces were collected into a sterile freezing vial weighing 2 ml, and immediately snap-frozen in liquid nitrogen. For bacterial DNA extraction, DNA was extracted and purified following the manufacture’s protocol using the EIANamp stool DNA kit (TIANGEN, DP328-02).

Microbiota 16S rRNA gene sequencing

Fecal samples, ileum contents, and colon contents were collected from wildtype, Chil1$^{-/-}$ littermates, or Villin-cre, IEC$^{\Delta Chil1}$ littermates and immediately frozen in liquid nitrogen. The microbial genomic DNA was extracted and 16S rRNA sequencing was performed by Biomarker Technologies. The hypervariable regions V3 and V4 of the bacterial 16S rRNA gene were sequenced using universal primers that flank these regions V3 (338F 5'-ACTCCTACGGGAGGCAGCA-3') and V4 (806R 5'-GGACTACHVGGGTWTCTAAT-3’). The sequencing was done using the IIIumina Sequencing platform. The resulting 16S rRNA gene sequences were analyzed using scripts from the BMK Cloud platform (www.biocloud.net). The microbial classification was performed using the SILVA138 and hierarchical clustering algorithms. The OTUs were determined by clustering the sequences with 97% similarity and were classified into different taxonomic ranks. The relative abundance of each

499 bacterial species was visualized using R software. The raw 16S rRNA gene sequencing data can be
500 accessed on the BMKCloud platform under the project ID
501 Microbial_updateReport_20211221092022313.
502
503 **16S qPCR analysis**
504 Quantitative PCR was performed using SYBR green master mix (Thermo Fisher, A25742) in
505 triplicates. This was done on a Real-Time PCR QuatStudio1 with accompanying software, following
506 the instructions provided by the manufacturer (Life Technologies, Grand Island, NY, USA). The
507 abundance of specific bacterial groups in the intestine was determined using qPCR with either
508 universal or bacteria-specific 16S rRNA gene primers. Standard curves were constructed with
509 *E.Coli OP50* 16S rRNA gene, which was amplified using conserved 16S rRNA primers. It should
510 be noted that qPCR measures the number of 16S gene copies per sample, not the actual bacterial
511 numbers or colony forming units. Primer sequences are provided in table S2.
512
513 **Table S2**
514 **qPCR primers**

Targeted bacteria	Primer No.	Sequence
Universal	27F	AGAGTTTGATCCTGGCTCAG
	1492R	GGTTACCTTGTTACGACTT
Gram-positive	928F–firm	TGAAACTYAAGGAATTGACG
	1040-firmR	ACCATGCACCACCTGTC
Lactobacillus	F	TGGAAACAGGTGCTAATACCG
	R	GTCCATTGTGGAAGATTCCC

515
516 **Key source tables**
517
518 **Antibodies and chemicals**

Reagent or Antibodies	Source	Indentifier
Dextran Sulfate Sodium Salt	MP	CAS:9011-18-1
AB-PAS staining kit	Solarbio	G1285
EIANamp stool DNA kit	TIANGEN	DP328-02
PAGE Gel Fast Preparation Kit	Shanghai Epizyme biotechnology	PG113
gel extraction kit	Omega--	D2500-02
SYBR Green kit	Thermo Fisher	A25742
hematoxylin	Servicebio	G1004
eosin	Biosharp	BL703b
DAB Substrate Kit	ZSGB-BIO	zli-9018
Tris	Solarbio	77-86-1
Sodium chloride	Solarbio	7647-14-5
disodium salt dihydrate (EDTA)	Sangon Biotech	6381-92-6
Sodium dodecyl sulfate (SDS)	BBI	A601336-0500
egtazic acid,Glycol ether diamine tetraacetic acid (EGTA)	BBI	67-42-5
TritonX-100	BBI	9002-93-1
Citric acid	Sangon Biotech	77-92-9
Vancomycin	Solarbio	V8050
Ampicillin- Sodium salt	Solarbio	A8180)
Metronidazole	Solarbio	M8060
Neomyein Sulfate	Solarbio	N8090
MRS broth	Solarbio	M8540

Goat serum	Solarbio	
Anti-Chi3l1 Polyclonal Antibody	Invitrogen	PA5-95897
Cha-A antibody	Santa Cruz	sc-393941
anti-mouse Chi3l1 Purified Rat Monoclonal IgG	R&D	MAB2649
MUC2 Polyclonal Antibody	Invitrogen	PA5-103083
Gram Positive Bacteria LTA Monoclonal Antibody (G43J)	Invitrogen	MA1-7402
488-conjugated Affinipure Goat Anti-Rabbit	Jackson	111-545-003
immunoresearch Alexa Fluor 594 AffiniPure Goat Anti-Mouse IgG (H+L)	Jackson	115-585-003
Goat anti-Rabbit IgG (H+L) Secondary Antibody-Biotin	Invitrogen	65-6140
Horseradish Peroxidase conjugate antibody	Invitrogen	A2664
Rabbit anti-Chi3l1 antibody	Proteintech	12036-1-AP
Goat anti-Rabbit IgG	Jackson ImmunoResearch	111-035-0030
Mouse anti-α-tubulin antibody	sigma	T5168
Goat anti-mouse IgG	Jackson ImmunoResearch	115-035-003
Goat anti-Rat IgG	Jackson ImmunoResearch	112-035-003
DAPI	Beyotime	c1006
Antifade mounting medium	Vectashield	H-1000-10
FDAA	5TAMRA; CHINESE PEPTIDE	CS-11-00433
gram-positive bacteria 16S rRNA probe	Guangzhou Exon Biotech	

Cell lines/ Bacteria strains

DLD-1 cells	a gift from Dr. Sun Jianwei at Yunnan University	
Staphylococcus saprophyticus	ATCC	15305
E. faecalis	ATCC	33186
Lactobacillus reuteri	ATCC	23272
E. coli strain *K12*	Dharmacon	Cat #OEC5042
E. coli strain *OP50*	CGC	RRID:WB STRAIN:OP50
Staphylococcus Sciuri	identified from C57BL/6J wild-type mice stools	citation: Kirienko NV, Cezairliyan BO, Ausubel FM, Powell JR. Pseudomonas aeruginosa PA14 pathogenesis in Caenorhabditis elegans. Methods Mol Biol. 2014;1149:653-669. doi:10.1007/978-1-4939-0473-0_50
E. coli	identified from C57BL/6J wild-type mice stools	

Statistical analysis

Data were presented as mean ± SEM. Statistical analyses were carried out using GraphPad Prism (GraphPad Software). Comparisons between two groups were carried out using unpaired Student t test. Comparisons among multiple groups (n>=3) were carried out using one-way ANOVA. P values

are as labeled and less than 0.05 was considered not significant. Patient data were analyzed by Mann-Whitney test.

Author Contributions

Y.C. and R.Z.Y. performed experiments, analyzed data, and wrote the manuscript. B.Q. organized and designed the study. Z.S. initiated, organized, designed the study and wrote the manuscript.

Acknowledgements

We thank Qun Lu (Yunnan University) for providing Villin-cre mice. We thank Wenxiang Fu (Yunnan University) for imaging technical support. We thank Jianwei Sun (Yunnan University) for providing DLD-1 cell line. We thank Zehan Hu (Shanghai Jiao Tong University) for methods of bacteria 16S FISH staining. This work was supported by National Natural Science Foundation of China (32071129 to Z.S., 32170794 to B.Q.), Yunnan Fundamental Research Projects (202101AT070022, 202001AW070006 to Z.S., 2019FY003022, 202001AV070011, 202001AW070006, 202201AT070196 to B.Q.), Ministry of Science and Technology of China (2019YFA0803100, 2019YFA0802100 to B.Q.).

Declaration of interests

The authors declare no competing interests.

Reference

1. Lozupone, C.A., et al., *Diversity, stability and resilience of the human gut microbiota.* Nature, 2012. **489**(7415): p. 220-230.
2. Charbonneau, M.R., et al., *A microbial perspective of human developmental biology.* Nature, 2016. **535**(7610): p. 48-55.
3. Sonnenburg, J.L. and F. Backhed, *Diet-microbiota interactions as moderators of human metabolism.* Nature, 2016. **535**(7610): p. 56-64.
4. Thaiss, C.A., et al., *The microbiome and innate immunity.* Nature, 2016. **535**(7610): p. 65-74.
5. Honda, K. and D.R. Littman, *The microbiota in adaptive immune homeostasis and disease.* Nature, 2016. **535**(7610): p. 75-84.
6. Baumler, A.J. and V. Sperandio, *Interactions between the microbiota and pathogenic bacteria in the gut.* Nature, 2016. **535**(7610): p. 85-93.
7. Petersen, C. and J.L. Round, *Defining dysbiosis and its influence on host immunity and disease.* Cellular Microbiology, 2014. **16**(7): p. 1024-1033.
8. Lee, J.Y., R.M. Tsolis, and A.J. Baumler, *GUT PHYSIOLOGY The microbiome and gut homeostasis.* Science, 2022. **377**(6601): p. 44-+.
9. McDonald, J.E., J.R. Marchesi, and B. Koskella, *Application of ecological and evolutionary theory to microbiome community dynamics across systems.* Proceedings of the Royal Society B-Biological Sciences, 2020. **287**(1941).
10. Gordon, J.I., *Honor Thy Gut Symbionts Redux.* Science, 2012. **336**(6086): p. 1251-1253.

11. Fu, J.X., et al., *Loss of intestinal core 1-derived O-glycans causes spontaneous colitis in mice.* Journal of Clinical Investigation, 2011. **121**(4): p. 1657-1666.
12. Johansson, M.E.V., et al., *The inner of the two Muc2 mucin-dependent mucus layers in colon is devoid of bacteria.* Proceedings of the National Academy of Sciences of the United States of America, 2008. **105**(39): p. 15064-15069.
13. Swidsinski, A., et al., *Spatial organization and composition of the mucosal flora in patients with inflammatory bowel disease.* Journal of Clinical Microbiology, 2005. **43**(7): p. 3380-3389.
14. Johansson, M.E.V., et al., *Bacteria penetrate the normally impenetrable inner colon mucus layer in both murine colitis models and patients with ulcerative colitis.* Gut, 2014. **63**(2): p. 281-291.
15. Gevers, D., et al., *The Treatment-Naive Microbiome in New-Onset Crohn's Disease.* Cell Host & Microbe, 2014. **15**(3): p. 382-392.
16. Donaldson, G.P., et al., *Gut microbiota utilize immunoglobulin A for mucosal colonization.* Science, 2018. **360**(6390): p. 795-800.
17. Lee, C.G., et al., *Role of chitin and chitinase/chitinase-like proteins in inflammation, tissue remodeling, and injury.* Annu Rev Physiol, 2011. **73**: p. 479-501.
18. Houston, D.R., et al., *Structure and ligand-induced conformational change of the 39-kDa glycoprotein from human articular chondrocytes.* Journal of Biological Chemistry, 2003. **278**(32): p. 30206-30212.
19. Fulde, M., et al., *Neonatal selection by Toll-like receptor 5 influences long-term gut microbiota composition.* Nature, 2018. **560**(7719): p. 489-493.
20. Vaishnava, S., et al., *The antibacterial lectin RegIIIgamma promotes the spatial segregation of microbiota and host in the intestine.* Science, 2011. **334**(6053): p. 255-8.
21. Groussin, M., F. Mazel, and E.J. Alm, *Co-evolution and Co-speciation of Host-Gut Bacteria Systems.* Cell Host Microbe, 2020. **28**(1): p. 12-22.
22. Hill, D.R., et al., *Bacterial Colonization Stimulates a Complex Physiological Response in the Immature Human Intestinal Epithelium.* In Vitro Cellular & Developmental Biology-Animal, 2018. **54**: p. S6-S6.
23. Zhao, T., et al., *Chitinase-3 like-protein-1 function and its role in diseases.* Signal Transduct Target Ther, 2020. **5**(1): p. 201.
24. Wang, W., et al., *Assessing the viability of transplanted gut microbiota by sequential tagging with D-amino acid-based metabolic probes.* Nat Commun, 2019. **10**(1): p. 1317.
25. Deutschmann, C., et al., *Identification of Chitinase-3-Like Protein 1 as a Novel Neutrophil Antigenic Target in Crohn's Disease.* Journal of Crohns & Colitis, 2019. **13**(7): p. 894-904.
26. Breyne, K., et al., *Immunomodulation of Host Chitinase 3-Like 1 During a Mammary Pathogenic Escherichia coli Infection.* Frontiers in Immunology, 2018. **9**.
27. Dela Cruz, C.S., et al., *Chitinase 3-like-1 promotes Streptococcus pneumoniae killing and augments host tolerance to lung antibacterial responses.* Cell Host Microbe, 2012. **12**(1): p. 34-46.
28. Mizoguchi, E., *Chitinase 3-like-1 exacerbates intestinal inflammation by enhancing bacterial adhesion and invasion in colonic epithelial cells.* Gastroenterology, 2006. **130**(2): p. 398-411.
29. Zhou, J.X., et al., *Breaking down the cell wall: Still an attractive antibacterial strategy.*

Frontiers in Microbiology, 2022. **13**.

30. Fusetti, F., et al., *Crystal structure and carbohydrate-binding properties of the human cartilage glycoprotein-39.* Journal of Biological Chemistry, 2003. **278**(39): p. 37753-37760.

31. Ferrandon, S., et al., *A single surface tryptophan in the chitin-binding domain from Bacillus circulans chitinase A1 plays a pivotal role in binding chitin and can be modified to create an elutable affinity tag.* Biochimica Et Biophysica Acta-General Subjects, 2003. **1621**(1): p. 31-40.

32. Ranok, A., et al., *Structural and Thermodynamic Insights into Chitooligosaccharide Binding to Human Cartilage Chitinase 3-like Protein 2 (CHI3L2 or YKL-39).* Journal of Biological Chemistry, 2015. **290**(5): p. 2617-2629.

33. Johansson, M.E.V., J.M.H. Larsson, and G.C. Hansson, *The two mucus layers of colon are organized by the MUC2 mucin, whereas the outer layer is a legislator of host-microbial interactions.* Proceedings of the National Academy of Sciences of the United States of America, 2011. **108**: p. 4659-4665.

34. Hu, Z.H., et al., *Small proline-rich protein 2A is a gut bactericidal protein deployed during helminth infection.* Science, 2021. **374**(6568).

35. Raimondi, S., et al., *Identification of mucin degraders of the human gut microbiota.* Scientific Reports, 2021. **11**(1).

36. Glover, J.S., T.D. Ticer, and M.A. Engevik, *Characterizing the mucin-degrading capacity of the human gut microbiota.* Scientific Reports, 2022. **12**(1).

37. Qin, J.J., et al., *A human gut microbial gene catalogue established by metagenomic sequencing.* Nature, 2010. **464**(7285): p. 59-U70.

659 **Figure 1**

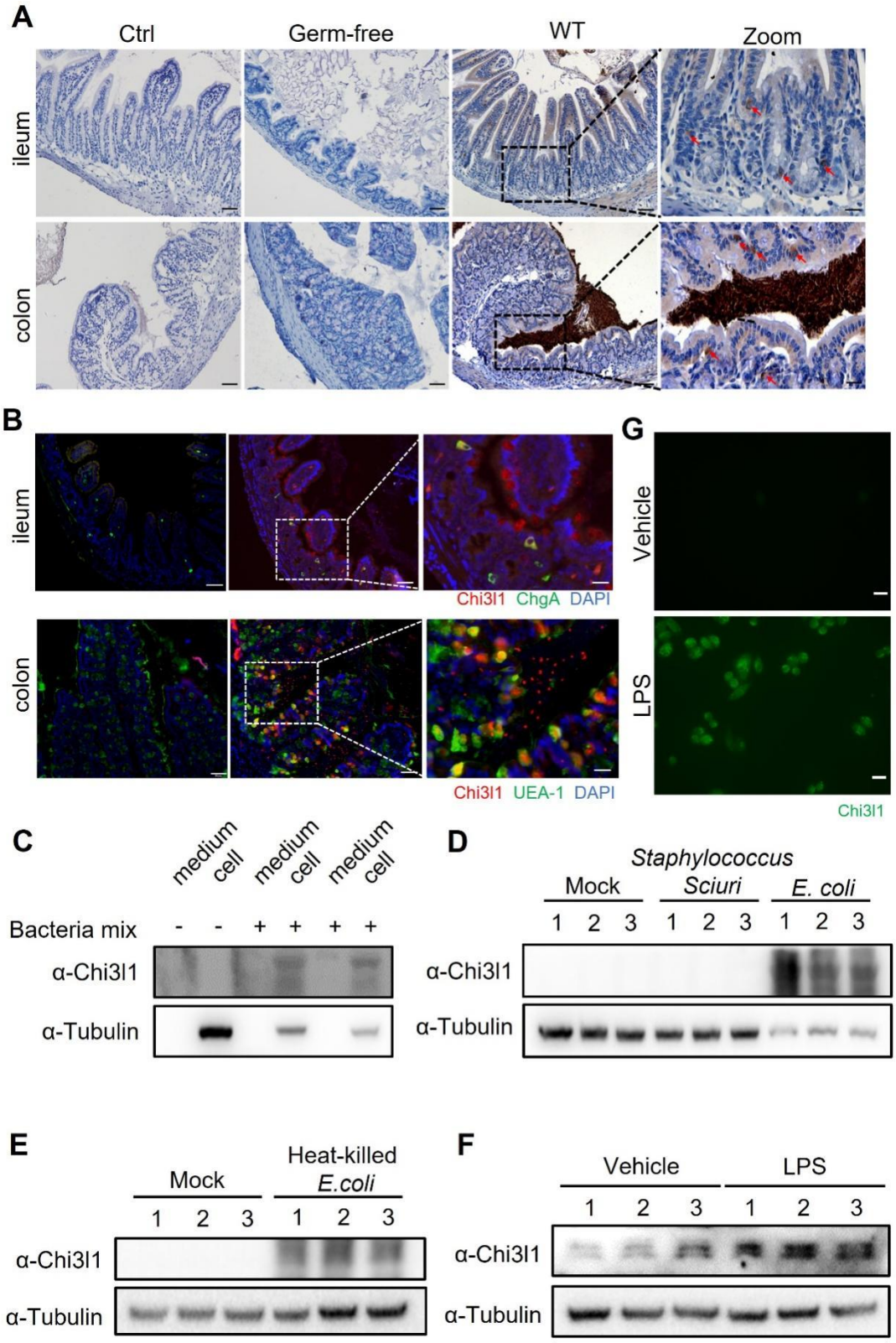

660
661

662 **Figure 1. Intestinal epithelial cells express Chi3l1 induced by gut microbiota.**

663 **(A)** IHC staining to detect Chi3l1 in both ileum and colon from germ-free and wildtype mice. Ctrl
664 (wildtype mice without application of first antibody), WT (wildtype C57B/6J mice). Red arrows

indicate Chi3l1-expressing cells. Scale bar, 50μm (Ctrl, Germ-free, WT) and 20μm(zoom). **(B)** Ileum and colon were collected from wildtype mice and stained with ChgA (green), Chi3l1(red), and nuclear DAPI (blue) in ileum and UEA-1 (green), Chi3l1(red), and nuclear DAPI (blue) in colon. Scale bar, 20μm. Ctrl (without application of first antibody), WT (wildtype C57B/6J mice). **(C)** Western blot to detect Chi3l1 protein expression in DLD-1 cells after bacteria mix infection for 12 hour. Bacteria mix are total bacteria extracted from feces of wildtype mice. **(D)** Western blot to detect Chi3l1 protein expression in DLD-1 cells after *Staphylococcus Sciuri* and *E. coli* infection for 12 hour. *Staphylococcus Sciuri* and *E. coli* are isolated from bacteria mix and verified by 16S rRNA sequencing. Three independent experimental results are showed. **(E)** Western blot to detect Chi3l1 protein expression in DLD-1 cells after treatment with heat-killed *E. coli* for 12 hour. Three independent experimental results are showed. **(F)** Western blot to detect Chi3l1 protein expression in DLD-1 cells after treatment with 100 pg/ml LPS for 12 hour. Three independent experimental results are showed. **(G)** Immunofluorescence to detect Chi3l1 protein expression in DLD-1 cells after treatment with 100pg/ml LPS for 12 hour. Scale bar, 20μm. All data above represent at least three independent experiments. Representative images are shown in A,B, n=3-4 mice/group.

Figure 2

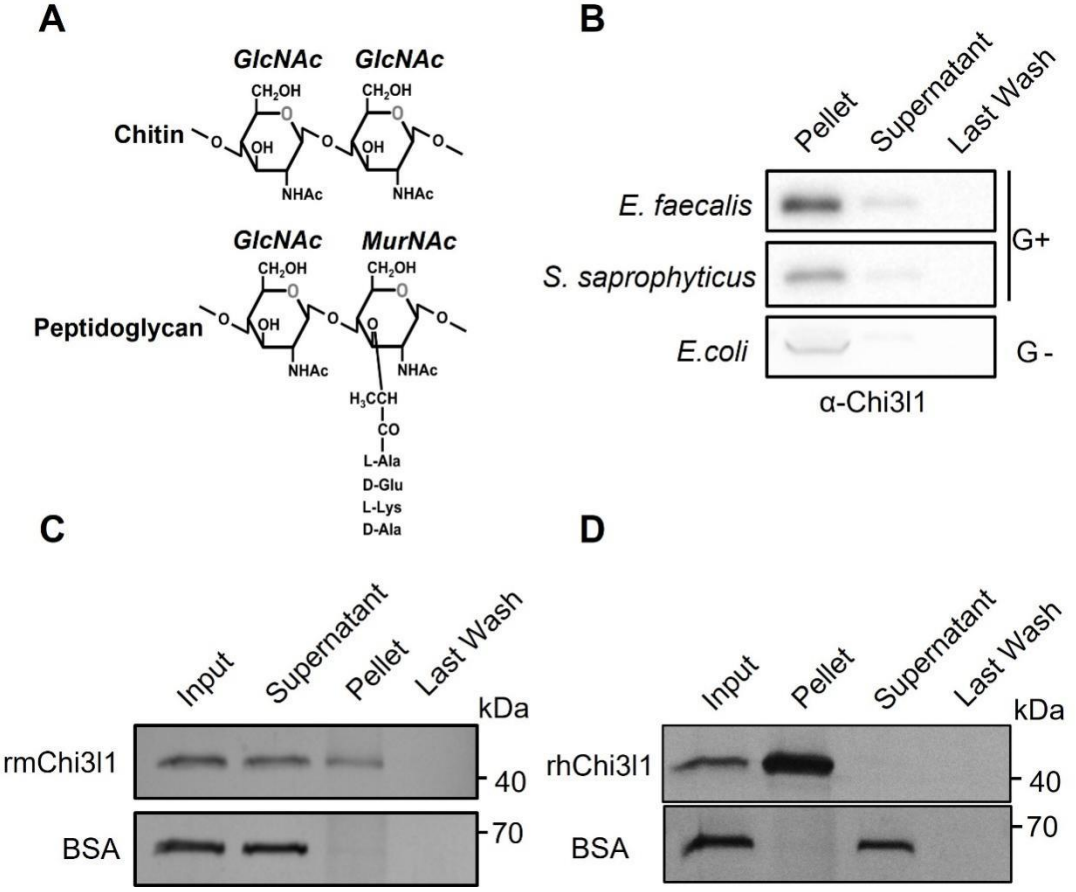

Figure 2. Chi3l1 interact with bacteria via peptidoglycan.

(A) Structural comparison between Chitin and peptidoglycan. **(B)** Gram-positive bacteria (*E.faecalis*, *S.saprophyticus*) and Gram-negative bacteria (*E.coli*) were incubated with 1μg of recombinant mouse Chi3l1 protein(rmChi3l1), respectively. Proteins bound to indicated bacteria were precipitated by centrifugation. Western blot was used to detect rmChi3l1 in Pellet, Supernatant (unbound proteins) and Last Wash (last wash unbound proteins). **(C)** Insoluble Peptidoglycan (PGN) were incubated with either recombinant mouse Chi3l1 protein (rmChi3l1) or Bovine serum albumin (BSA). Proteins bound to PGN were precipitated by centrifugation. Silver staining was used to detect rmChi3l1 in Input, Supernatant (unbound proteins), Pellet and Last Wash (last wash unbound proteins). **(D)** Insoluble Peptidoglycan (PGN) were incubated with recombinant human Chi3l1 protein (rhChi3l1). Proteins bound to PGN were precipitated by centrifugation. Silver staining was used to detect rhChi3l1 in Input, Supernatant (unbound proteins), Pellet and Last Wash (last wash unbound proteins). All data above represent at least three independent experiments.

Figure 3

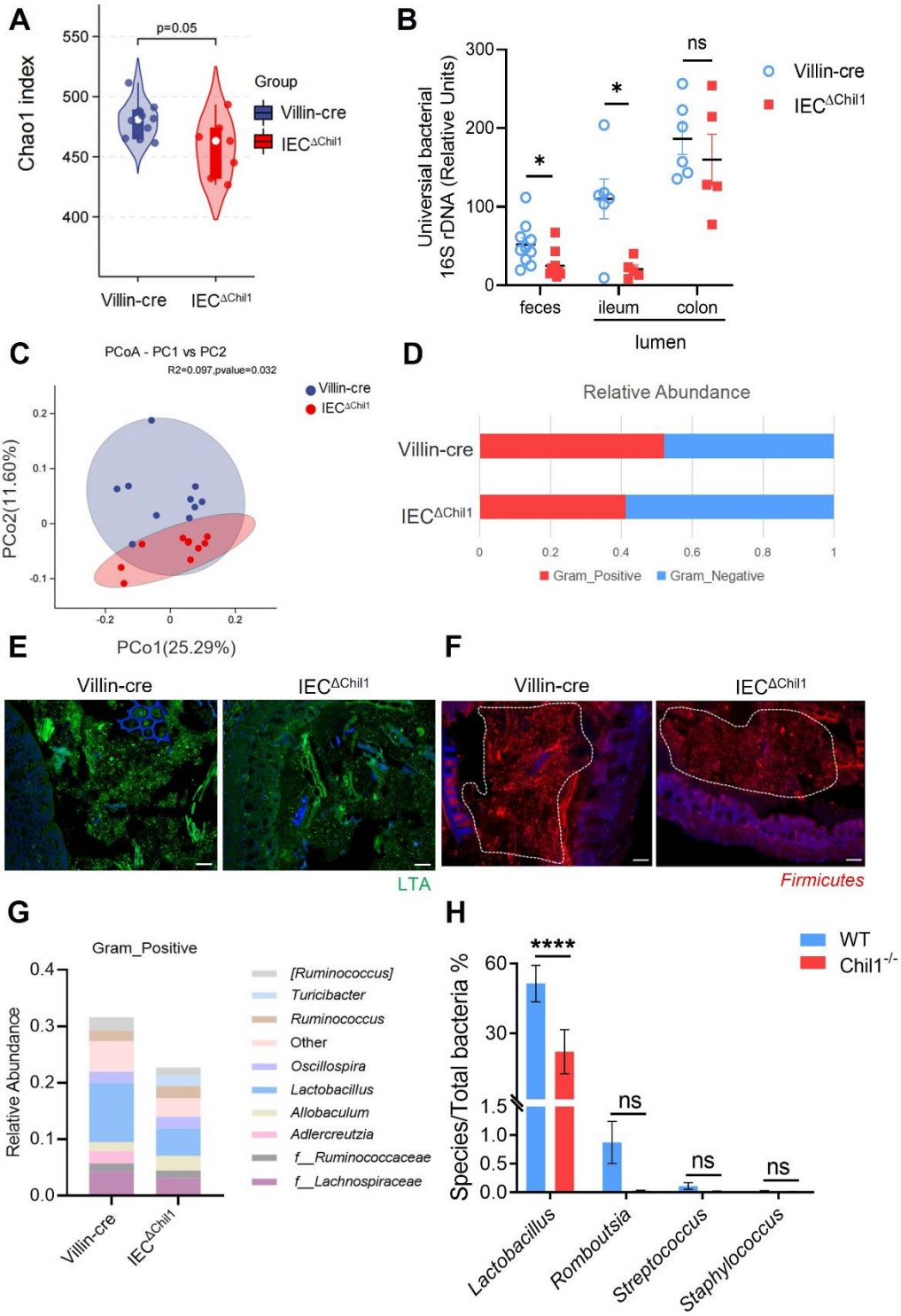

Figure 3. Intestinal bacteria are disordered in IEC$^{\Delta Chil1}$ mice, especially Gram-positive bacteria.

(A, C, D, G) Female Villin-cre and IEC$^{\Delta Chil1}$ littermates continue to cage together after weaning for 8 weeks. Microbial communities in feces and intestinal lumen were characterized by 16S rRNA sequencing. n=7 or 10/group. **(A)** Alpha diversity analysis of colon contents between Villin-cre and IEC$^{\Delta Chil1}$ littermates. **(B)** qPCR analysis of total bacteria in the feces and ileum, colon luminal microbial communities of Villin-cre and IEC$^{\Delta Chil1}$ littermates. Values for each bacterial group are

expressed relative to total 16S rRNA levels. Mean ± SEM is displayed. Two-tailed, unpaired student t-test was performed. *P<0.05, ns, not significant. n=5-10/group. **(C)** Principal Component Analysis of weighed UniFrac distances of 16S community profiles of Villin-cre and IEC$^{\Delta Chil1}$ littermates feces (binary-jaccard). **(D)** Relative abundance of Gram-positive and Gram-negative bacteria in colon contents of Villin-cre and IEC$^{\Delta Chil1}$ littermates are shown. **(E)** LTA (green) was detected by immunofluorescence in colon sections of Villin-cre and IEC$^{\Delta Chil1}$ littermates. Nuclei were detected with DAPI. Scale bar, 50μm. **(F)** Fluorescence in situ hybridization (FISH) detection of gram-positive bacteria (red) in the colon of Villin-cre and IEC$^{\Delta Chil1}$ littermates, nuclei were detected with DAPI (blue). Scale bars, 50um. **(G)** Relative abundance of Gram-positive bacteria genera in colon lumen of Villin-cre and IEC$^{\Delta Chil1}$ littermates. **(H)** Female wildtype and Chil1$^{-/-}$ littermates continue to cage together after weaning for 8 weeks. Microbial communities in feces were characterized by 16S rRNA sequencing. Mean ± SEM is displayed. Two-tailed, unpaired student t-test was performed. ****P<0.0001, ns, not significant. n=4 or 6/group. Representative images are shown in E, F, n= 3/4 mice/group.

773 **Figure 4**

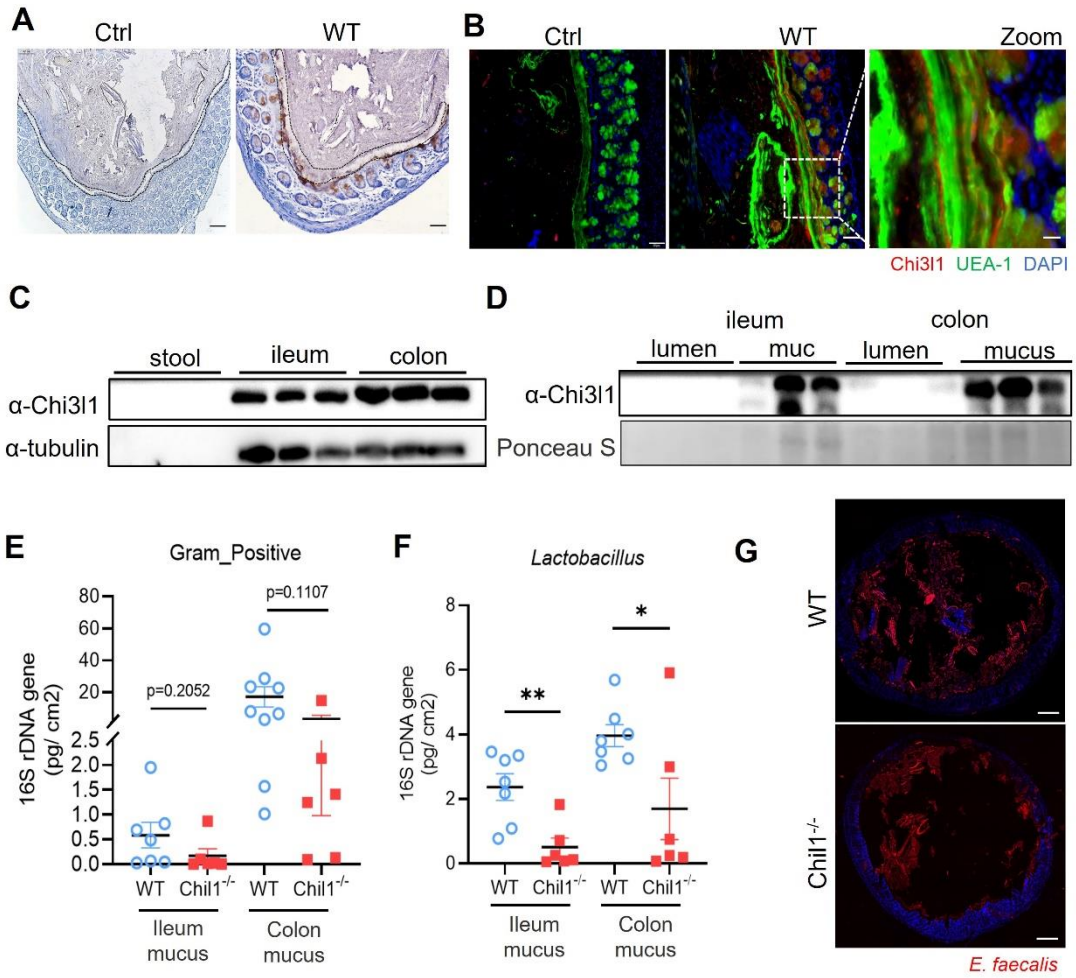

774

775 **Figure 4. Chi3l1 promotes the colonization of Gram-positive bacteria in intestinal mucus layer.**
776 **(A)** IHC staining to detect Chi3l1 in colon mucus layer from wildtype mice. Ctrl (without
777 application of ant-Chi3l1 antibody), WT (wildtype C57B/6J mice). Black dotted line outlines mucus
778 layer. Scale bar, 50μm (Ctrl, WT). **(B)** Colons were collected from wildtype mice and stained with
779 UEA-1 (green), Chi3l1(red), and nuclear DAPI (blue). Ctrl (without application of first antibody),
780 WT (wildtype C57B/6J mice). Scale bars, 50um (Ctrl, WT) and 20μm(zoom). **(C)** Stool, ileum and
781 colon tissues were collected from wildtype mice. Western blot was used to detect Chi3l1 expression
782 in these samples. n=3 mice/sample. **(D)** Both luminal and mucus-associated proteins of either ileum
783 or colon were extracted. Western blot was used to detect Chi3l1 expression in these samples. lumen
784 (luminal proteins), mucus (mucus-associated proteins). n=3 mice/sample. **(E&F)** qPCR analysis of
785 specific bacteria in the ileum and colon mucus microbial communities of wildtype and Chil1$^{-/-}$
786 littermates. **(E)** qPCR analysis of Gram-positive bacteria is shown. **(F)** qPCR analysis of Gram-
787 positive bacteria is shown. Values for each bacterial group are expressed relative to total 16S rRNA
788 levels. WT (wildtype C57B/6J mice). Mean ± SEM is displayed. Two-tailed, unpaired student t-test
789 was performed. P value is as indicated in E. *P<0.05, **P<0.01, n=6-9/group. **(G)** Rectal injection
790 of both wildtype and Chi11$^{-/-}$ mice with FDAA-labeled *E. faecalis* (a Gram-positive bacteria strain)
791 for 4 hour. Colon sections were collected and colonization of *E.faecalis* was examined under
792 microscope. Nuclei were stained with DAPI. Representative images are shown in A, B, G, n=3-4
793 mice/group.

794 **Figure 5**

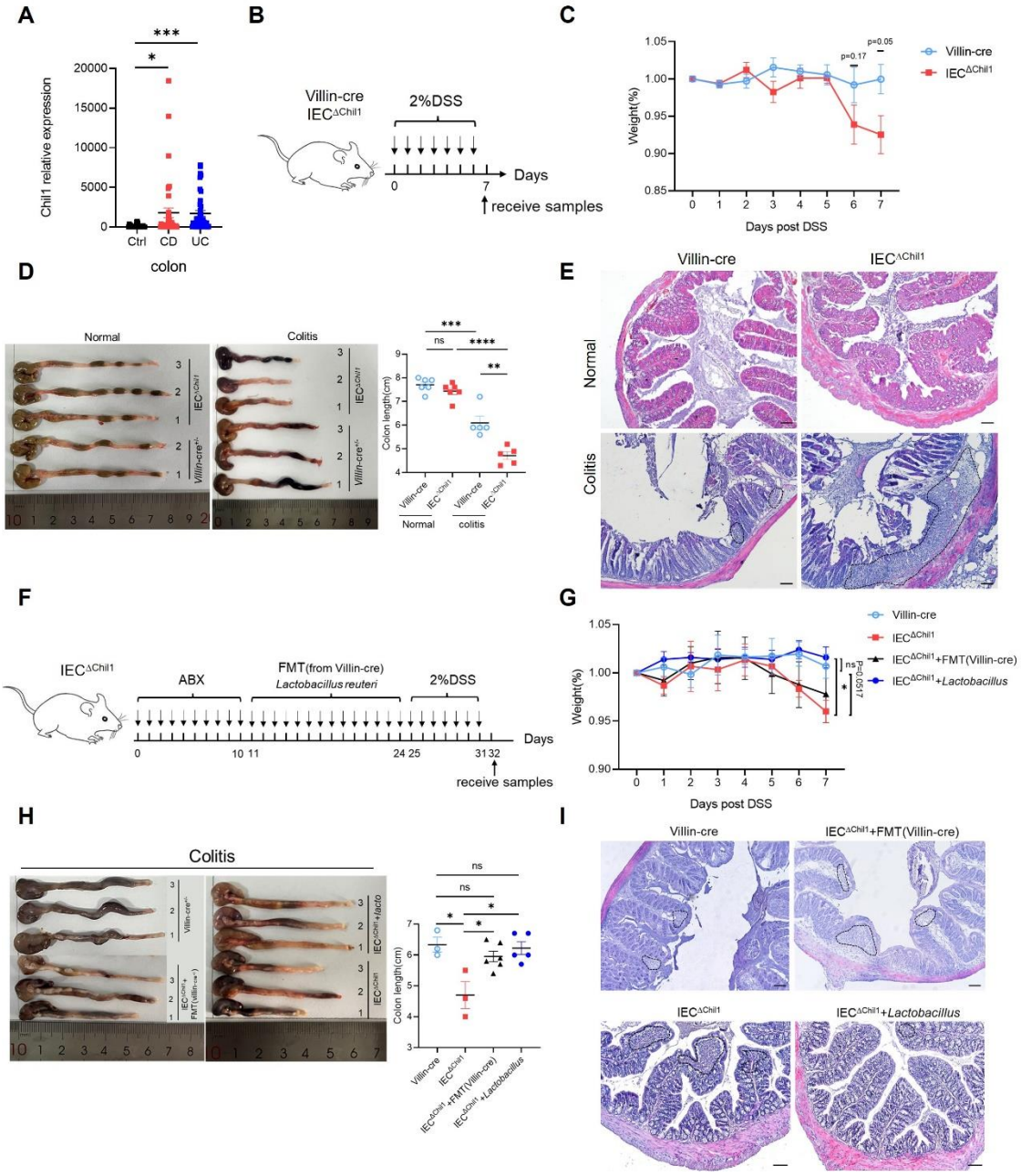

795

796 **Figure 5. Disordered intestinal bacteria in IEC$^{\Delta Chil1}$ mice contribute to IBD.**
797 **(A)** *Chil1* mRNA relative expression in colon tissues of patients without gut disease (controls, n=35)
798 or with Crohn's disease (CD, n=40), ulcerative colitis (UC, n=40), (GEO Datasets: SRP303290),
799 Mann-Whitney test was performed. *P < 0.05; ***P < 0.001. **(B)** Schematic model of the
800 experimental design. Both Villin-cre and IEC$^{\Delta Chil1}$ littermates were fed with 2% DSS in drinking
801 water to induce colitis. **(C)** Weight change of Villin-cre and IEC$^{\Delta Chil1}$ littermates during DSS feeding.
802 Weight (%) = Current weight/Initial weight. P values are as indicated. **(D)** Representative colonic
803 length from Normal and DSS-treated Villin-cre and IEC$^{\Delta Chil1}$ littermates (left) and the statistics of
804 colonic length (right) (**P < 0.01; ***P < 0.001; ****P < 0.0001, ns, not significant). **(E)** H&E
805 staining of mice colon from Normal and DSS-treated Villin-cre and IEC$^{\Delta Chil1}$ littermates. The
806 inflamed areas are outlined by white dotted line, Scale bars=100um. **(F)** Schematic of the

experimental design. First, antibiotics were used to eliminate gut microbiota for 10 days, and then either fecal microbiota from Villin-cre mice (FMT) or *Lactobacillus reuteri* were transplanted back *to* IEC$^{\Delta Chil1}$ mice orally every day for 2 weeks. Finally, colitis mouse model was constructed by 2% DSS feeding in drinking water for another 7 days. **(G-I)** Villin-cre and IEC$^{\Delta Chil1}$ were only fed with 2% DSS in drinking water for 7days. IEC$^{\Delta Chil1}$+FMT(Villin-cre), and IEC$^{\Delta Chil1}$+*Lactobacillus* were constructed as described in F. **(G)** Weight change of Villin-cre, IEC$^{\Delta Chil1}$, IEC$^{\Delta Chil1}$+FMT(Villin-cre), and IEC$^{\Delta Chil1}$+*Lactobacillus* mice during DSS feeding. **(H)** Representative colonic length from Villin-cre, IEC$^{\Delta Chil1}$, IEC$^{\Delta Chil1}$+FMT(Villin-cre), and IEC$^{\Delta Chil1}$+*Lactobacillus* mice (left) and the statistics of colonic length (right). Mean ± SEM is displayed in G, H. one-way ANOVA was performed. P value is as indicated. *P<0.05, ns, not significant, n=3-6/group. **(I)** H&E staining of mice colon from Villin-cre, IEC$^{\Delta Chil1}$, IEC$^{\Delta Chil1}$+FMT(Villin-cre), and IEC$^{\Delta Chil1}$+*Lactobacillus* mice after DSS treatment. The inflamed area is outlined by black dotted line, Scale bars=100um. Representative images are shown in C, E, H, I, n=3-6 mice/group.

Figure 6

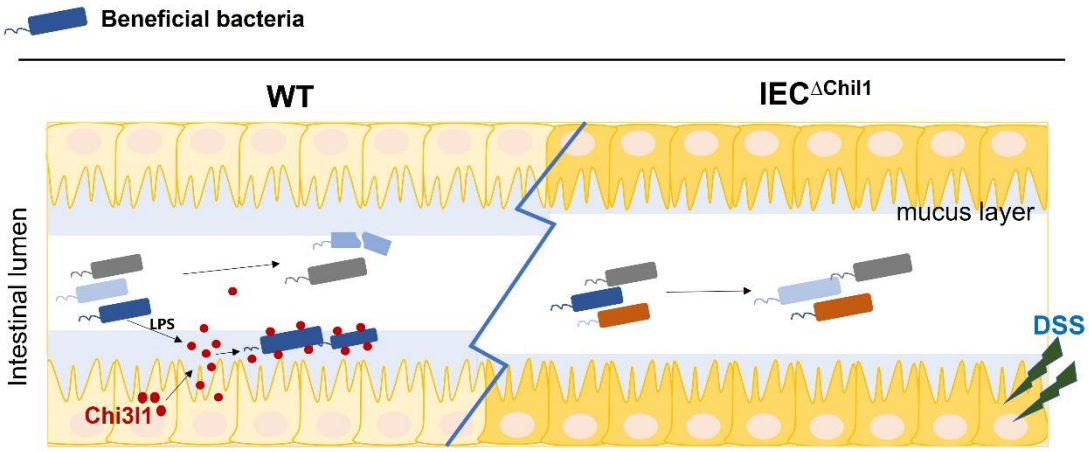

Figure 6. A schematic working model. Intestinal epithelial cells are stimulated by the gut microbiota to express Chi3l1. Once expressed, Chi3l1 is secreted into the mucus layer where it interacts with the gut microbiota, specifically through a component of bacterial cell walls called peptidoglycan. This interaction between Chi3l1 and bacteria is beneficial for the colonization of bacteria in the mucus, particularly for gram-positive bacteria like *Lactobacillus*. Moreover, a deficiency of Chi3l1 leads to an imbalance in the gut microbiota, which exacerbates colitis induced by dextran sodium sulfate (DSS).

884 **Supplemental figures**

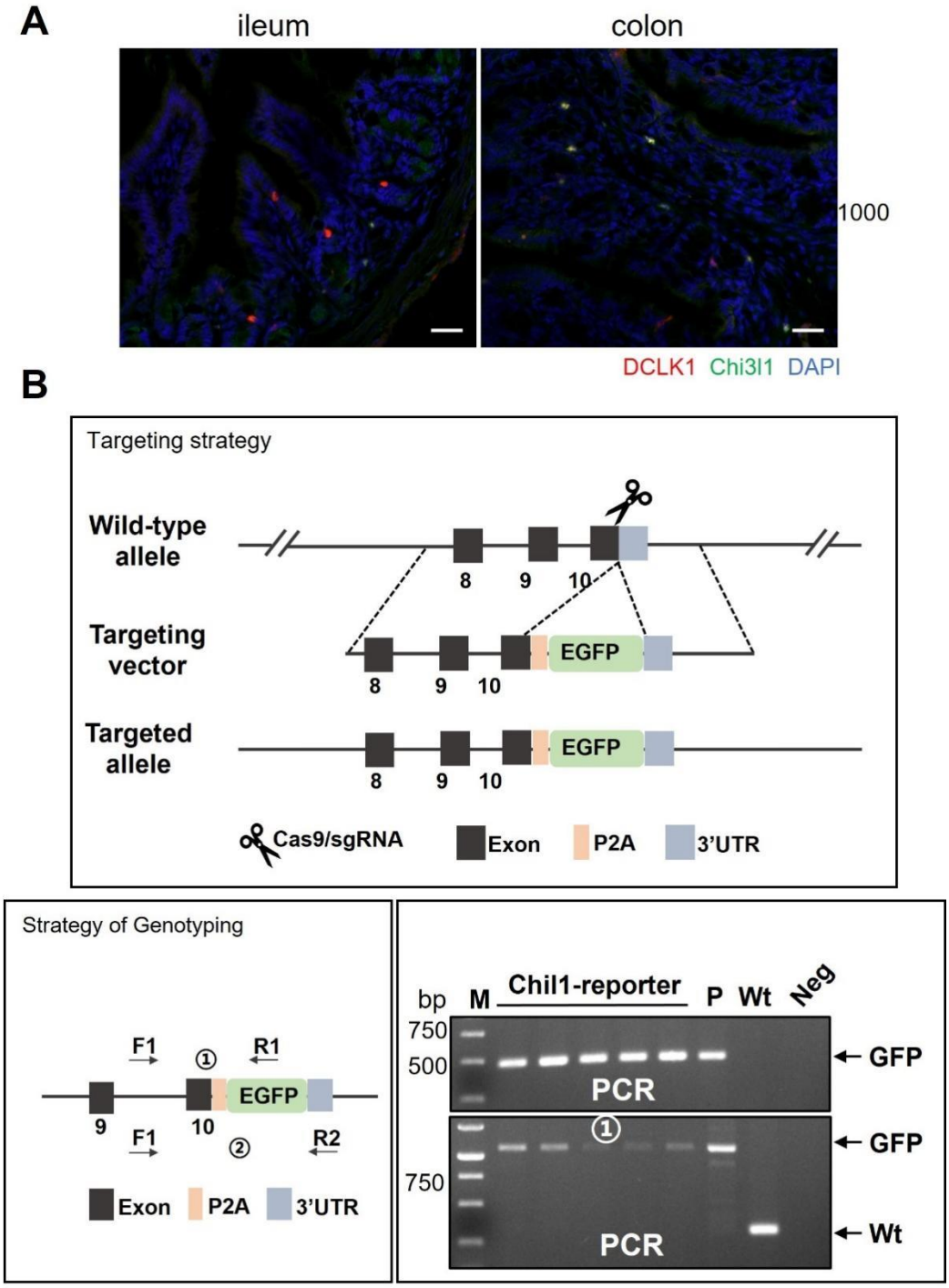

885

886 **Supplementary Fig. 1 Chi3l1 don't express in tuft cells.**
887 (A) Ileum and colon were collected from Chil1-EGFP reporter mice and stained with DCLK1 (red),
888 Chi3l1(green), and nuclear DAPI (blue). Scale bar, 20μm. Representative images are shown, n=3
889 mice/group. (B) The construction, genotyping strategy, and genotyping results of Chil1-EGFP
890 reporter mice. P: positive control; Wt: Wild-type control; Neg: Blank control(ddH2O); M: DNA
891 Ladder.

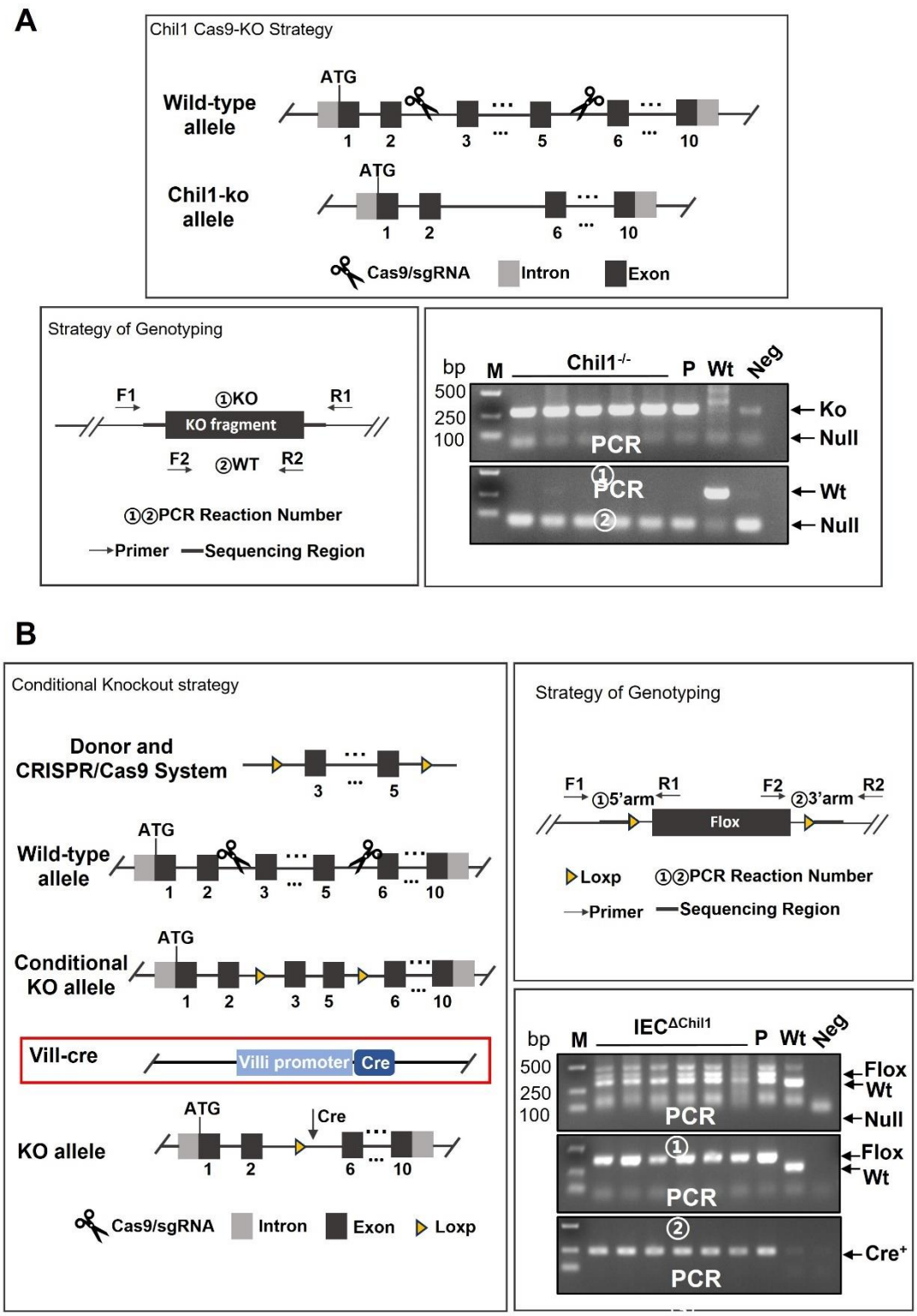

Supplementary Fig. 2 The construction and genotype of Chi3l1$^{-/-}$ and IEC$^{\Delta Chil1}$ mice.

(A) The construction, genotyping strategy and genotyping results of Chil1$^{-/-}$ mice. P: positive control; Wt: Wild-type control; Neg: Blank control(ddH2O); M: DNA Ladder.

(B) The construction, genotyping strategy and genotyping results of IEC$^{\Delta Chil1}$ mice. P:positive control; Wt: Wild-type control; Neg: Blank control(ddH2O); M: DNA Ladder. PCR① and ② implicated flox, ③implicated cre.

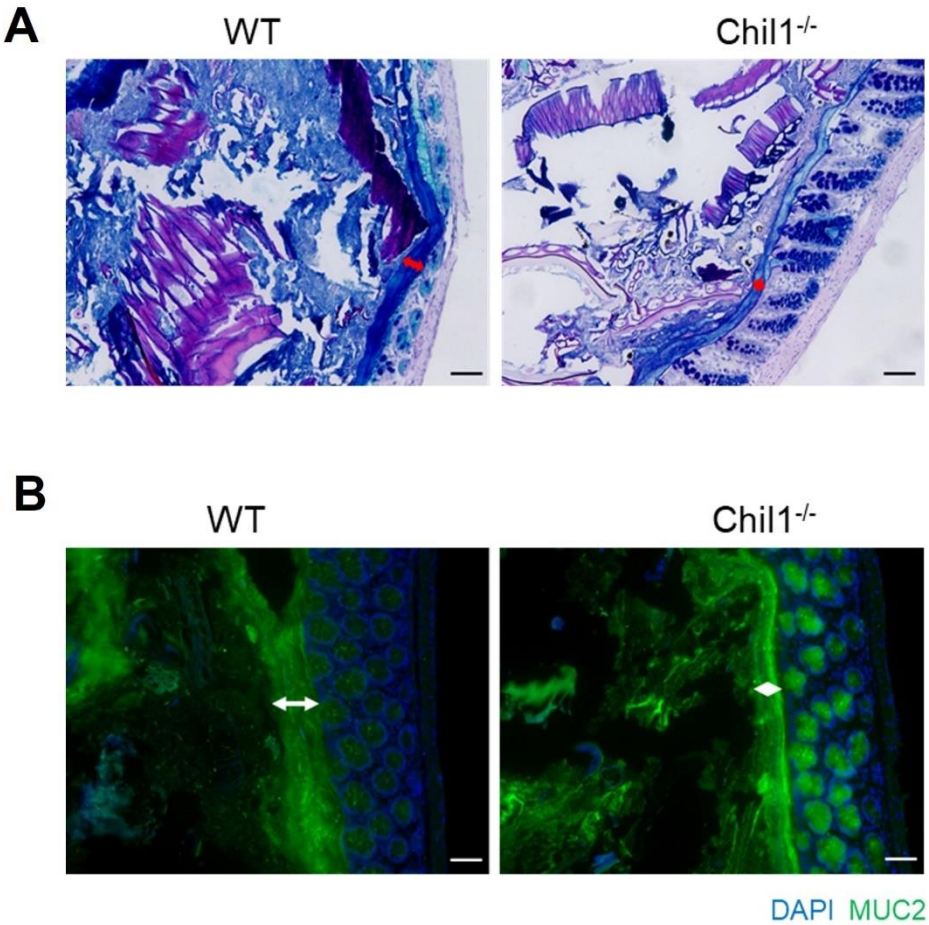

Supplementary Fig. 3 Chil1$^{-/-}$ mice possess shortening mucus layer.
(A) Periodic acid-Schiff and Alcian blue (AB-PAS) staining in the colons of WT and Chil1$^{-/-}$ littermates. Scale bars, 100μm. **(A)** Immunofluorescence staining to detect Mucin 2 (green) and nuclear DAPI (blue) in colon from WT and Chil1$^{-/-}$ littermates. Scale bar, 50μm. Representative images are shown in A, B, n=6 mice/group.

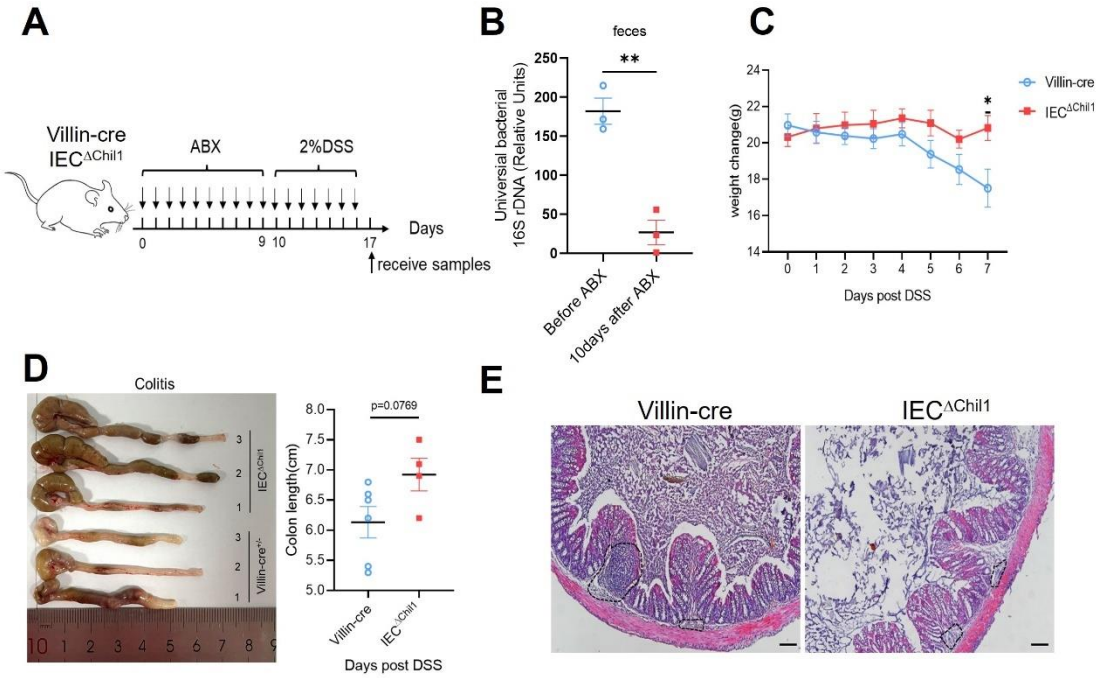

Supplementary Fig. 4 Chi3l1-mediated bacteria, but not Chi3l1 itself affect more upon the development of colitis.

(A) Schematic model of the experimental design. Both Villin-cre and IEC$^{\Delta Chil1}$ littermates were fed with 2% DSS in drinking water to induce colitis after elimination of gut microbiota by antibiotics for 10 days. **(B)** qPCR analysis of total bacteria in the feces of Villin-cre and IEC$^{\Delta Chil1}$ littermates. Values for each bacterial group are expressed relative to total 16S rRNA levels. Mean ± SEM is displayed. Two-tailed, unpaired student t-test was performed. **P<0.01, n=3/group. **(C)** Weight change of Villin-cre and IEC$^{\Delta Chil1}$ mice during DSS feeding. **(D)** Representative colonic length from Colitis Villin-cre and IEC$^{\Delta Chil1}$ mice (left) and the statistics of colonic length (right). Mean ± SEM is displayed. Two-tailed, unpaired student t-test was performed. P value is as indicated. **(E)** H&E staining of colitis mice colon from Villin-cre and IEC$^{\Delta Chil1}$. The inflamed area is outlined by black dotted lines, Scale bars=100 μm. n=4-6 mice/group.

Figure 1

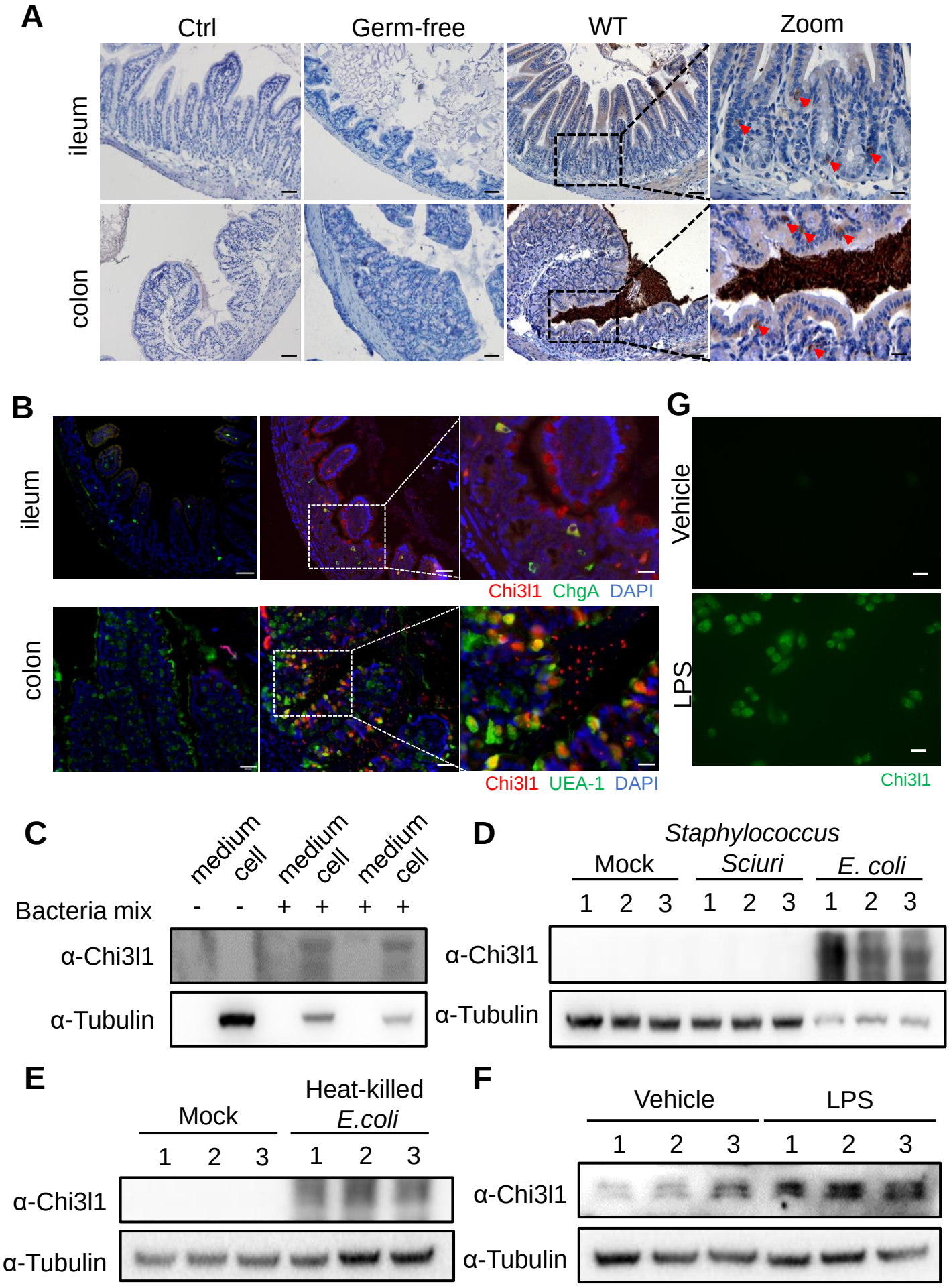
A
Ctrl
Germ-free
WT
Zoom
ileum
colon
B
ileum
colon
Chi3l1 ChgA DAPI
Chi3l1 UEA-1 DAPI
G
Vehicle
LPS
Chi3l1
C
medium
cell
medium
cell
medium
cell
Bacteria mix
- - + + + +
α-Chi3l1
α-Tubulin
D
Staphylococcus
Mock
Sciuri
E. coli
1 2 3 1 2 3 1 2 3
α-Chi3l1
α-Tubulin
E
Mock
Heat-killed
E.coli
1 2 3 1 2 3
α-Chi3l1
α-Tubulin
F
Vehicle
LPS
1 2 3 1 2 3
α-Chi3l1
α-Tubulin

Figure 2

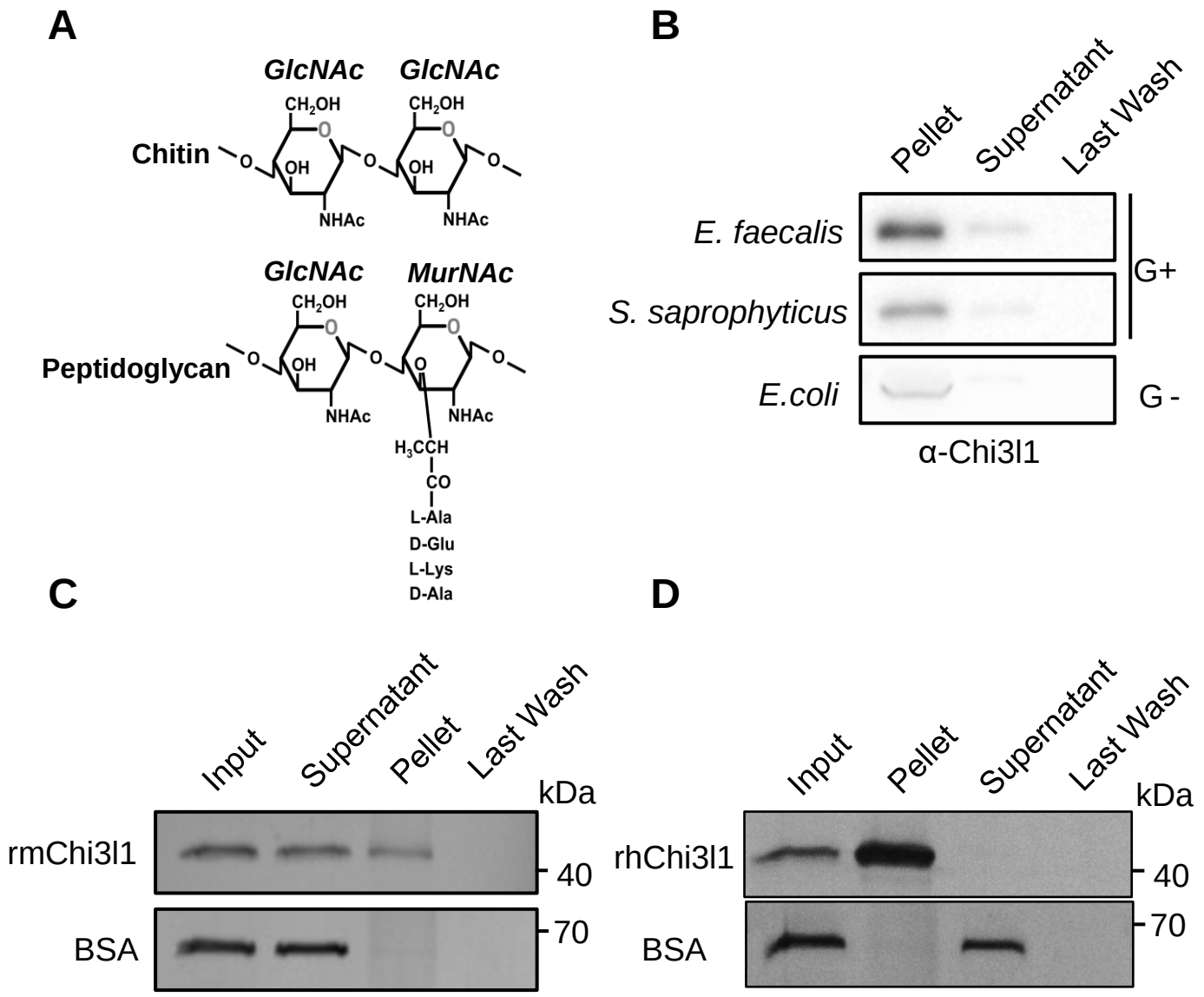
A
GlcNAc
GlcNAc
Chitin
CH2OH
OH
NHAc
GlcNAc
MurNAc
Peptidoglycan
H3CCH
CO
L-Ala
D-Glu
L-Lys
D-Ala
B
Pellet
Supernatant
Last Wash
E. faecalis
S. saprophyticus
E.coli
G+
G -
α-Chi3l1
C
Input
Supernatant
Pellet
Last Wash
kDa
rmChi3l1
BSA
40
70
D
Input
Pellet
Supernatant
Last Wash
kDa
rhChi3l1
BSA
40
70

Figure 3

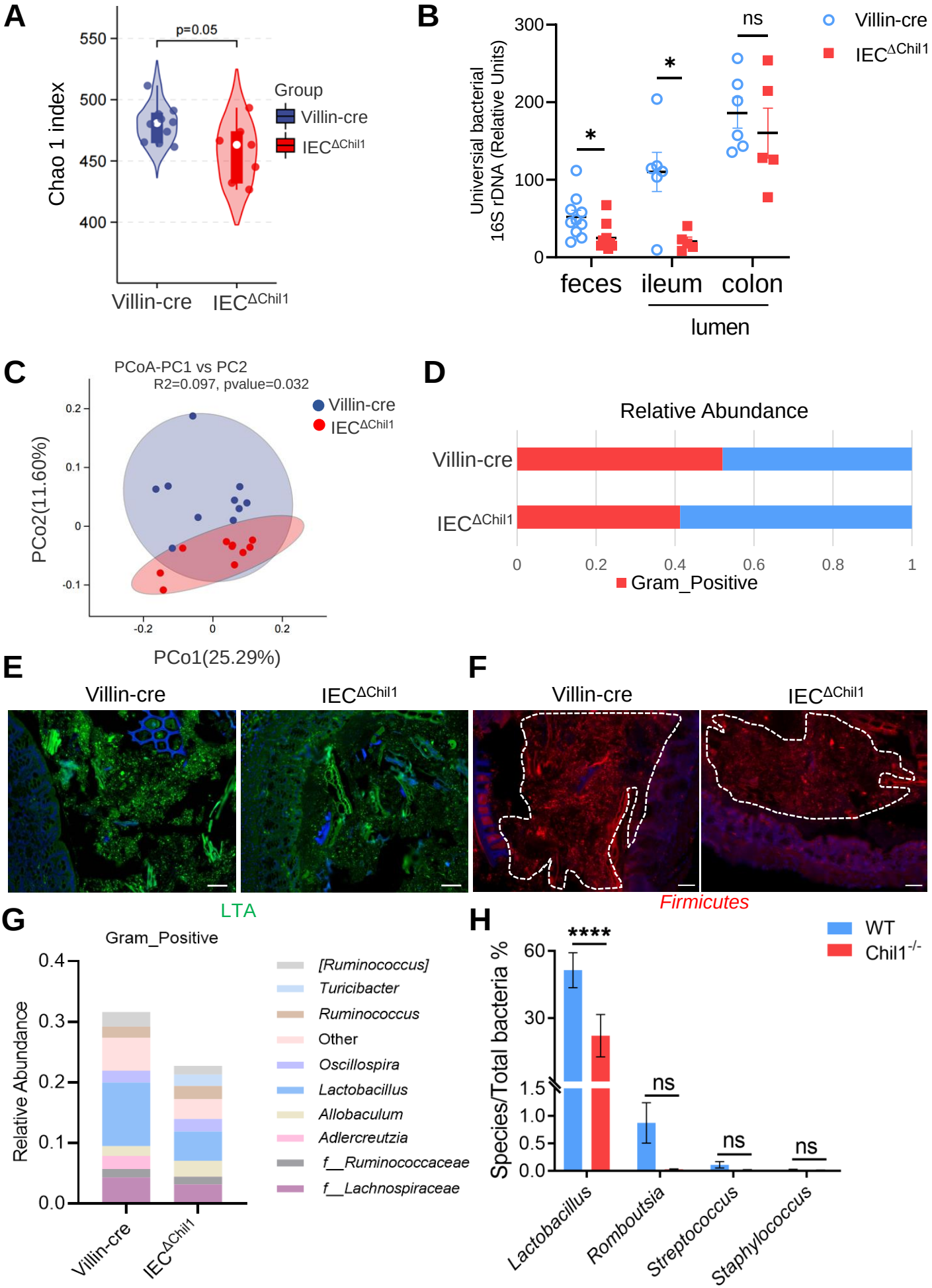
A
p=0.05
Chao 1 index
550
500
450
400
Group
Villin-cre
IEC$^{\Delta Chil1}$
Villin-cre
IEC$^{\Delta Chil1}$
B
Universal bacterial 16S rDNA (Relative Units)
300
200
100
0
ns
*
*
Villin-cre
IEC$^{\Delta Chil1}$
feces
ileum
colon
lumen
C
PCoA-PC1 vs PC2
R2=0.097, pvalue=0.032
Villin-cre
IEC$^{\Delta Chil1}$
PCo2(11.60%)
0.2
0.1
0
-0.1
-0.2
0
0.2
PCo1(25.29%)
D
Relative Abundance
Villin-cre
IEC$^{\Delta Chil1}$
0
0.2
0.4
0.6
0.8
1
Gram_Positive
E
Villin-cre
IEC$^{\Delta Chil1}$
LTA
F
Villin-cre
IEC$^{\Delta Chil1}$
Firmicutes
G
Gram_Positive
Relative Abundance
0.4
0.3
0.2
0.1
0.0
Villin-cre
IEC$^{\Delta Chil1}$
[Ruminococcus]
Turicibacter
Ruminococcus
Other
Oscillospira
Lactobacillus
Allobaculum
Adlercreutzia
f__Ruminococcaceae
f__Lachnospiraceae
H
Species/Total bacteria %
60
30
1.5
1.0
0.5
0.0
****
ns
ns
ns
WT
Chil1$^{-/-}$
Lactobacillus
Romboutsia
Streptococcus
Staphylococcus

Figure 4

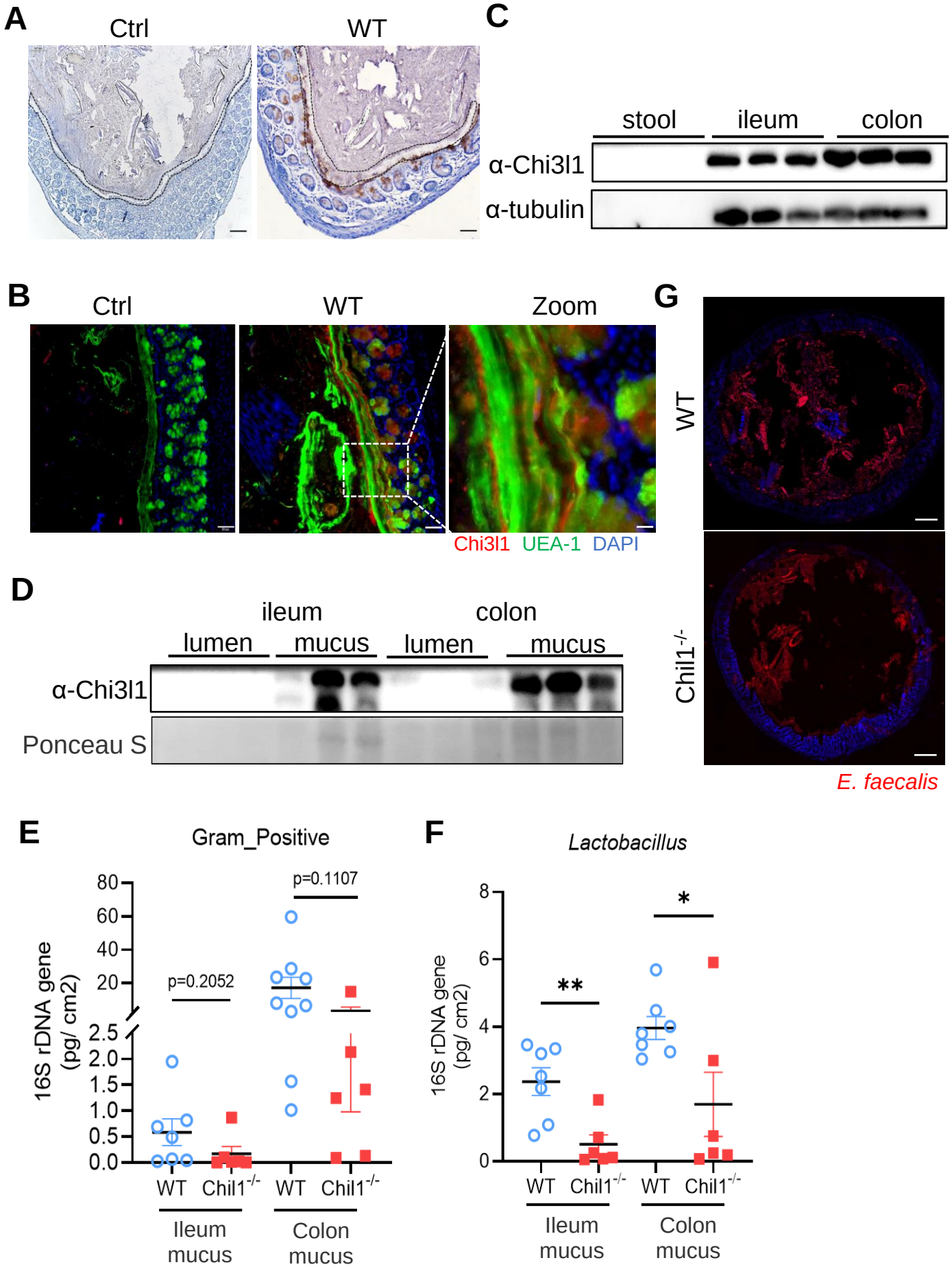
A
Ctrl
WT
C
stool
ileum
colon
α-Chi3l1
α-tubulin
B
Ctrl
WT
Zoom
Chi3l1 UEA-1 DAPI
G
WT
Chil1-/-
E. faecalis
D
ileum
colon
lumen
mucus
lumen
mucus
α-Chi3l1
Ponceau S
E
Gram_Positive
16S rDNA gene (pg/ cm2)
p=0.2052
p=0.1107
WT
Chil1-/-
WT
Chil1-/-
Ileum mucus
Colon mucus
F
Lactobacillus
16S rDNA gene (pg/ cm2)
**
*
WT
Chil1-/-
WT
Chil1-/-
Ileum mucus
Colon mucus

Figure 5

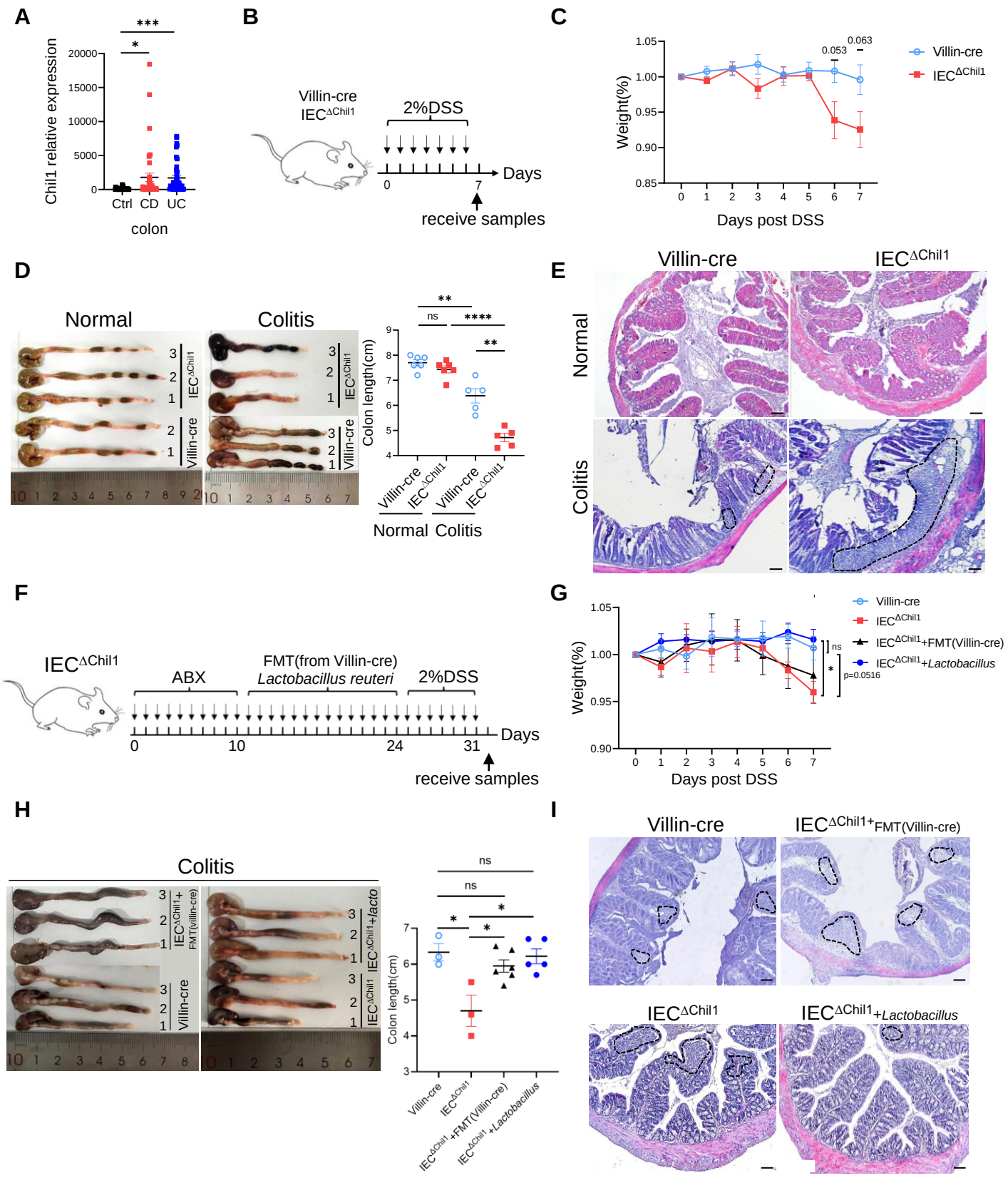
A
Chil1 relative expression
Ctrl CD UC
colon
B
Villin-cre
IEC^ΔChil1
2%DSS
Days
receive samples
C
Weight(%)
Villin-cre
IEC^ΔChil1
Days post DSS
D
Normal
Colitis
Colon length(cm)
Villin-cre
IEC^ΔChil1
Normal Colitis
E
Villin-cre
IEC^ΔChil1
Normal
Colitis
F
IEC^ΔChil1
ABX
FMT(from Villin-cre)
Lactobacillus reuteri
2%DSS
Days
receive samples
G
Weight(%)
Villin-cre
IEC^ΔChil1
IEC^ΔChil1+FMT(Villin-cre)
IEC^ΔChil1+Lactobacillus
p=0.0516
Days post DSS
H
Colitis
Colon length(cm)
Villin-cre
IEC^ΔChil1
IEC^ΔChil1+FMT(Villin-cre)
IEC^ΔChil1+Lactobacillus
I
Villin-cre
IEC^ΔChil1+FMT(Villin-cre)
IEC^ΔChil1
IEC^ΔChil1+Lactobacillus

Figure 6

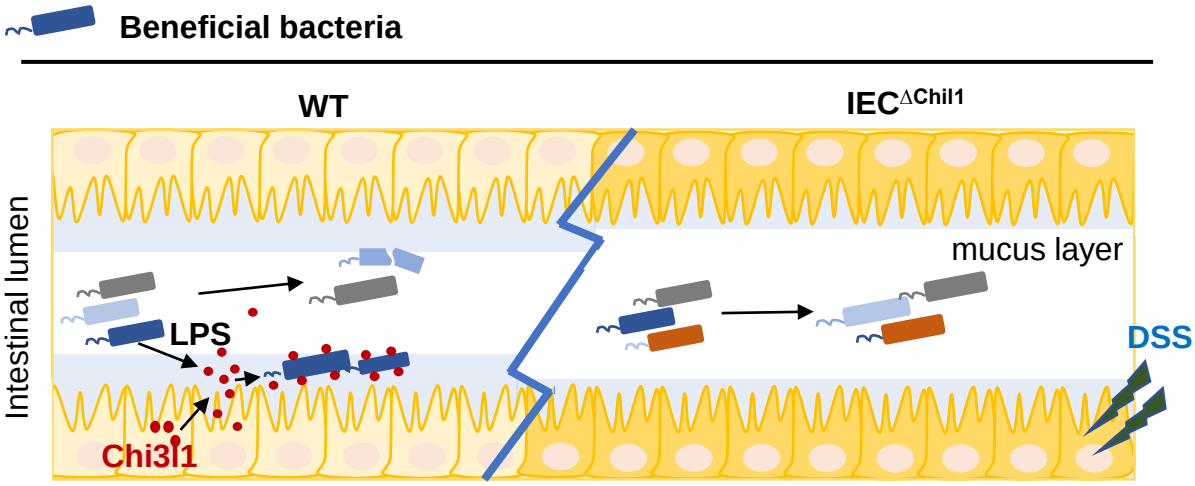
Beneficial bacteria
WT
IEC$^{\Delta Chil1}$
Intestinal lumen
mucus layer
LPS
DSS
Chi3l1

Supplemental Figures

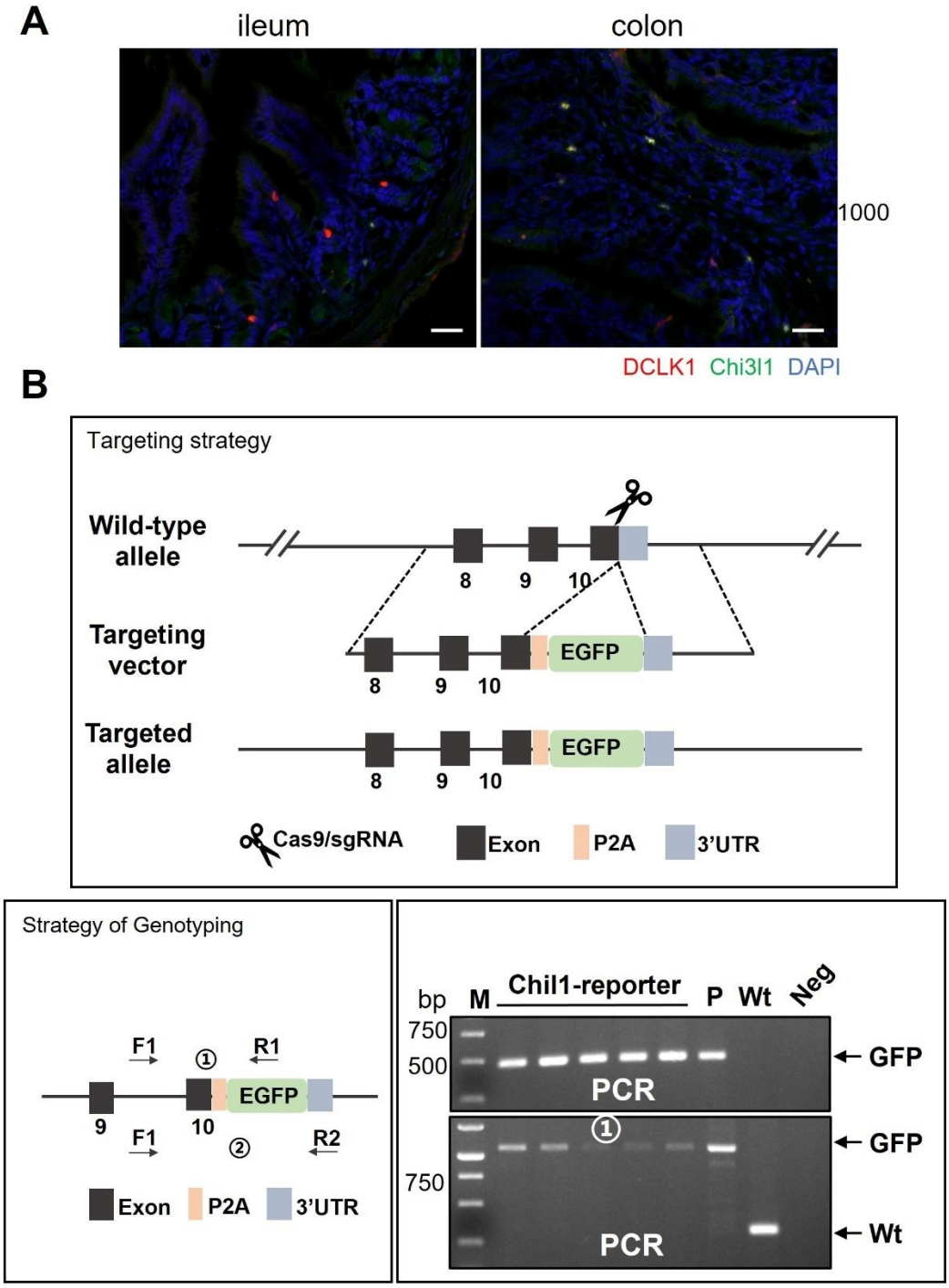

Supplementary Fig. 1 Chi3l1 don't express in tuft cells.
(A) Ileum and colon were collected from Chil1-EGFP reporter mice and stained with DCLK1 (red), Chi3l1(green), and nuclear DAPI (blue). Scale bar, 20μm. Representative images are shown, n=3 mice/group. (B) The construction, genotyping strategy, and genotyping results of Chil1-EGFP reporter mice. P: positive control; Wt: Wild-type control; Neg: Blank control(ddH2O); M: DNA Ladder.

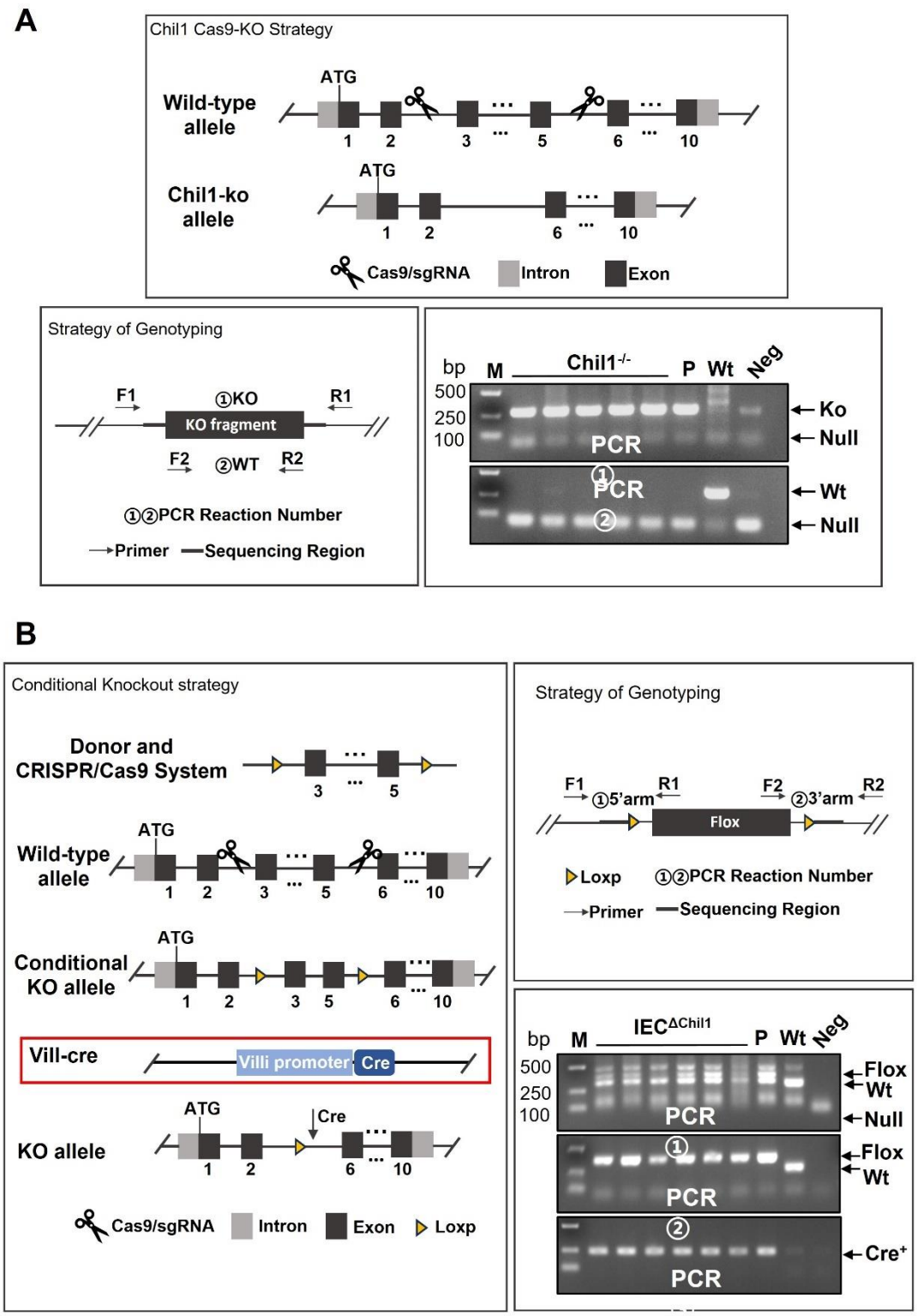

Supplementary Fig. 2 The construction and genotype of Chi3l1$^{-/-}$ and IEC$^{\Delta Chil1}$ mice.

(A) The construction, genotyping strategy and genotyping results of Chil1$^{-/-}$ mice. P: positive control; Wt: Wild-type control; Neg: Blank control(ddH2O); M: DNA Ladder.

(B) The construction, genotyping strategy and genotyping results of IEC$^{\Delta Chil1}$ mice. P:positive control; Wt: Wild-type control; Neg: Blank control(ddH2O); M: DNA Ladder. PCR① and ② implicated flox, ③implicated cre.

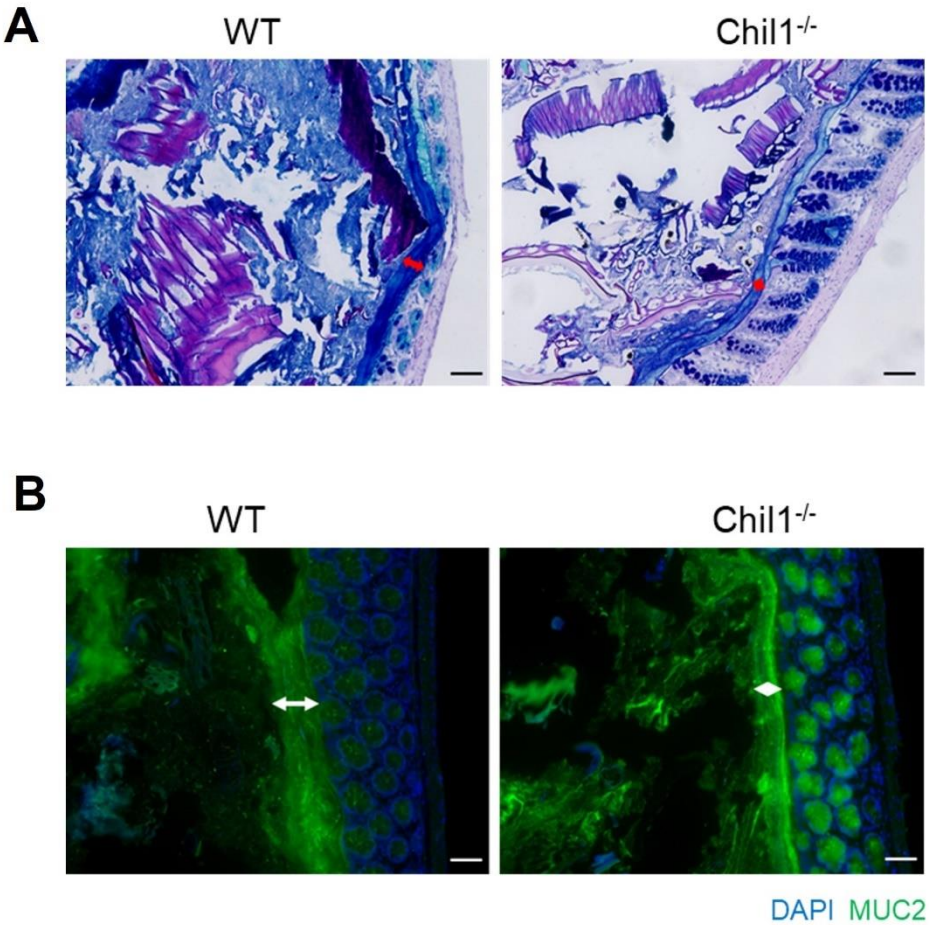

Supplementary Fig. 3 Chil1$^{-/-}$ mice possess shortening mucus layer.
(A) Periodic acid-Schiff and Alcian blue (AB-PAS) staining in the colons of WT and Chil1$^{-/-}$ littermates. Scale bars, 100μm. **(A)** Immunofluorescence staining to detect Mucin 2 (green) and nuclear DAPI (blue) in colon from WT and Chil1$^{-/-}$ littermates. Scale bar, 50μm. Representative images are shown in A, B, n=6 mice/group.

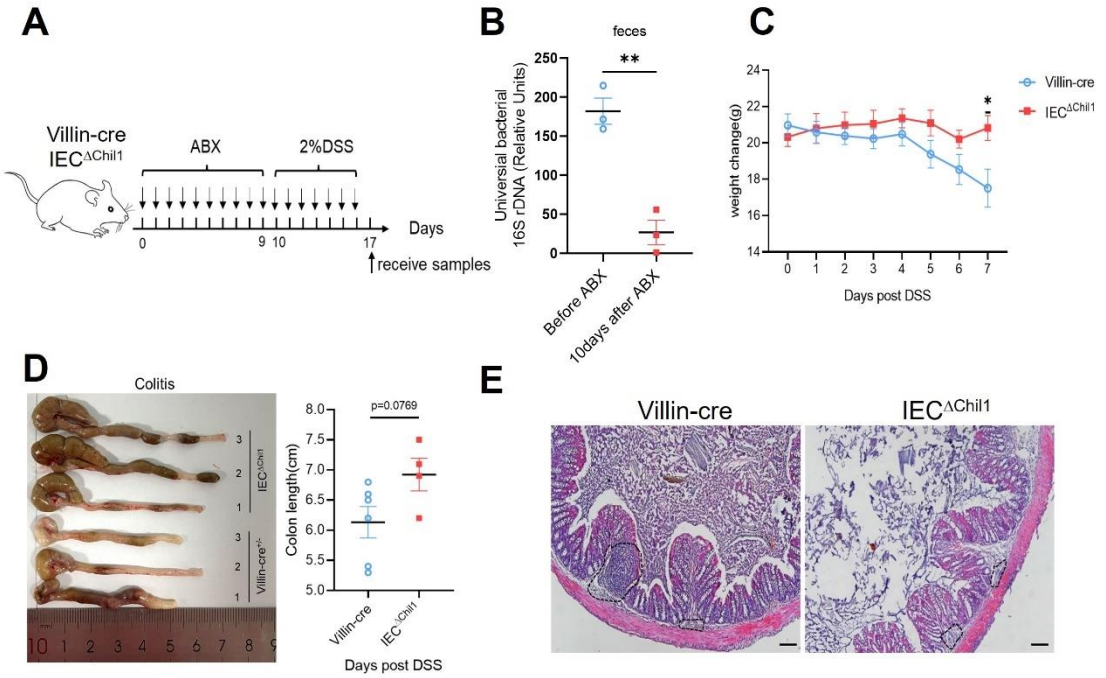

Supplementary Fig. 4 Chi3l1-mediated bacteria, but not Chi3l1 itself affect more upon the development of colitis.

(A) Schematic model of the experimental design. Both Villin-cre and IEC$^{\Delta Chil1}$ littermates were fed with 2% DSS in drinking water to induce colitis after elimination of gut microbiota by antibiotics for 10 days. **(B)** qPCR analysis of total bacteria in the feces of Villin-cre and IEC$^{\Delta Chil1}$ littermates. Values for each bacterial group are expressed relative to total 16S rRNA levels. Mean ± SEM is displayed. Two-tailed, unpaired student t-test was performed. **P<0.01, n=3/group. **(C)** Weight change of Villin-cre and IEC$^{\Delta Chil1}$ mice during DSS feeding. **(D)** Representative colonic length from Colitis Villin-cre and IEC$^{\Delta Chil1}$ mice (left) and the statistics of colonic length (right). Mean ± SEM is displayed. Two-tailed, unpaired student t-test was performed. P value is as indicated. **(E)** H&E staining of colitis mice colon from Villin-cre and IEC$^{\Delta Chil1}$. The inflamed area is outlined by black dotted lines, Scale bars=100 μm. n=4-6 mice/group.